Journal of
Materials Chemistry A

ROYAL SOCIETY
OF CHEMISTRY

REVIEW

View Article Online
View Journal | View Issue

Check for updates

Cite this: *J. Mater. Chem. A*, 2024, **12**, 33334

Green ammonia: revolutionizing sustainable energy for a carbon-free future

Zihao Zhang,†[ab] Hangjian Zhang,†[ab] Hongyu Jiang[ab] and Lu Li *[ab]

Ammonia (NH_3) plays a pivotal role in the transition toward sustainable energy systems. With its high hydrogen content, energy density, ease of storage and transport, and zero carbon emissions, ammonia has emerged as a promising energy carrier. While the conventional Haber–Bosch process remains the dominant method for NH_3 synthesis, new technologies driven by renewable energy sources are demonstrating greater efficiency and sustainability. Nonetheless, realizing the full potential of ammonia as an energy vector requires overcoming significant technical, economic, and environmental challenges across its lifecycle, including its production, storage, transportation, and application. This review provides a comprehensive analysis of recent advances in green ammonia synthesis and its energy applications, with particular emphasis on innovations in production technology, storage and transport solutions, and their environmental impacts. By summarizing recent research developments, this review aims to promote future advancements in ammonia technology and underscore its pivotal role in the global energy transition.

Received 15th October 2024
Accepted 29th October 2024

DOI: 10.1039/d4ta07339h

rsc.li/materials-a

1 Introduction

Ammonia, as a critical chemical feedstock, has had a profound impact on human society. The development of ammonia synthesis technology has significantly influenced global economic and social progress, serving as a cornerstone for modern agriculture. The invention of the Haber–Bosch process in the early 20th century enabled the large-scale production of nitrogen fertilizers, drastically reducing agricultural dependence on soil fertility and revolutionizing farming practices.[1] However, with increasing global emphasis on environmental protection and sustainability, the production and use of ammonia face new challenges and opportunities.

Since its inception in the early 20th century, the Haber–Bosch process has remained the dominant method for ammonia production worldwide.[2] Although highly efficient, this process operates under extreme conditions of high temperature and pressure, resulting in significant energy consumption and considerable carbon emissions.[3] With the escalating challenge of climate change, the search for low-carbon and energy-efficient ammonia synthesis technologies has become a priority. In recent years, researchers have focused

Zihao Zhang

Zihao Zhang received his BS in Chemistry from Henan Polytechnic University in 2020. He is currently a PhD candidate under the guidance of Prof. Lu Li at the State Key Laboratory of Inorganic Synthesis and Preparative Chemistry at Jilin University. His research focuses on plasma-catalytic ammonia synthesis.

Hangjian Zhang

Hangjian Zhang received his BS in Chemistry from Jilin University in 2023. He is currently an MS candidate at the State Key Laboratory of Inorganic Synthesis and Preparative Chemistry at Jilin University. His research focuses on ammonia decomposition for hydrogen production.

---

[a] *State Key Laboratory of Inorganic Synthesis and Preparative Chemistry, College of Chemistry, Jilin University, Changchun 130012, People's Republic of China. E-mail: luli@jlu.edu.cn*

[b] *College of Chemistry, Jilin University, Changchun 130012, People's Republic of China*

† Equal contributions.

on developing greener alternatives, such as electrocatalytic synthesis, solar-driven synthesis, and biocatalysis.[4] These emerging technologies not only reduce carbon emissions from ammonia production but also have the potential to lower costs and improve overall economic efficiency. However, the production, transportation, and use of ammonia may have environmental impacts, including potential ammonia leaks and disruption of ecosystems.[5] Therefore, the challenge is to advance ammonia technology while managing and minimizing its environmental impacts. To address these challenges, scientists need to conduct comprehensive life-cycle assessments of ammonia and develop effective environmental management strategies to ensure its sustainable use.[6]

Ammonia also holds great potential in the energy sector. It is considered an efficient hydrogen-storage medium as its liquid form is more efficient and safer to store and transport compared to gaseous hydrogen. Moreover, ammonia's potential as fuel has garnered widespread attention, with studies showing that it can be used in fuel cells and low-carbon power generation, contributing to the reduction in greenhouse gas emissions. Progress in this area will drive the hydrogen economy forward and play a significant role in the global energy transition.

In summary, ammonia has broad application potential in modern society, particularly in the energy sector. While traditional ammonia production methods present environmental concerns, advances in green synthesis technologies, the use of ammonia as a hydrogen carrier and fuel, and improvements in related technologies offer promising solutions to these challenges. This review systematically examines recent research advances in ammonia synthesis and utilization, with a focus on the development of green ammonia synthesis technologies, its applications in the energy sector, storage and transportation technologies, and their environmental impacts (Fig. 1). By summarizing and analyzing existing research, it aims to provide a scientific basis for future developments in ammonia technology and highlights its potential role in the global energy transition.

2 Physicochemical properties of ammonia

2.1 Basic properties of ammonia

Ammonia is a colorless gas with a strong, pungent odor, composed of nitrogen and hydrogen. It serves as a precursor in the synthesis of many important nitrogen compounds. The molecular geometry of ammonia is trigonal pyramidal, with the nitrogen atom at the center and three hydrogen atoms occupying the vertices of the triangular base. Due to the lone pair of electrons on the nitrogen atom, ammonia is highly polar, with the nitrogen atom carrying a partial negative charge and each hydrogen atom carrying a partial positive charge. Additionally, nitrogen forms covalent bonds with each hydrogen atom, sharing electrons to maintain the stability of the molecular structure. Ammonia has a melting point of −77 °C and a boiling point of −33.3 °C, which means it exists as a gas at room temperature and pressure. Furthermore, ammonia is highly soluble in water, forming ammonium hydroxide, which is strongly alkaline and widely used in laboratory and industrial applications. Ammonia contains a high hydrogen content of 17.6 wt%, making it a promising hydrogen-storage material.[7] Compared to hydrogen gas, ammonia is easier and more convenient to store and transport. Additionally, as a carbon-free energy carrier, ammonia burns completely to produce nitrogen and water, without emitting harmful gases, such as CO or CO_2.[8]

2.2 Storage and transportation characteristics of ammonia

A key requirement for an efficient hydrogen-storage carrier is ease of storage and transportation, which can facilitate its broad application and deployment. Ammonia can be stored in either liquid or gaseous form. Ammonia can be easily liquefied at room temperature and 0.86 MPa pressure or at atmospheric pressure and −33 °C. Its volumetric energy density of 12.7 MJ L^{-1} far exceeds that of liquid hydrogen (8.49 MJ L^{-1}).[9,10] Storing ammonia in liquid form can not only conserve storage space but also minimize leakage risks. Additionally, ammonia readily dissolves in water, forming an aqueous solution with

Hongyu Jiang

Hongyu Jiang received her BS in Chemistry from Jilin Normal University in 2023. She is currently an MS candidate at the State Key Laboratory of Inorganic Synthesis and Preparative Chemistry at Jilin University. Her research focuses on photocatalytic organic liquid hydrogen storage.

Lu Li

Lu Li studied chemistry at Jilin University (BS, 2006) and received his PhD in inorganic chemistry under Prof. Jiesheng Chen (2012). After completing his postdoctoral research with Prof. Chaojun Li at McGill University in Canada (2013–2017), he returned to Jilin University as a professor at the State Key Laboratory of Inorganic Synthesis and Preparative Chemistry (2017). His research interests include light-driven activation of inert small molecules (such as CH_4, N_2, and alkanes) and low-carbon conversion technologies.

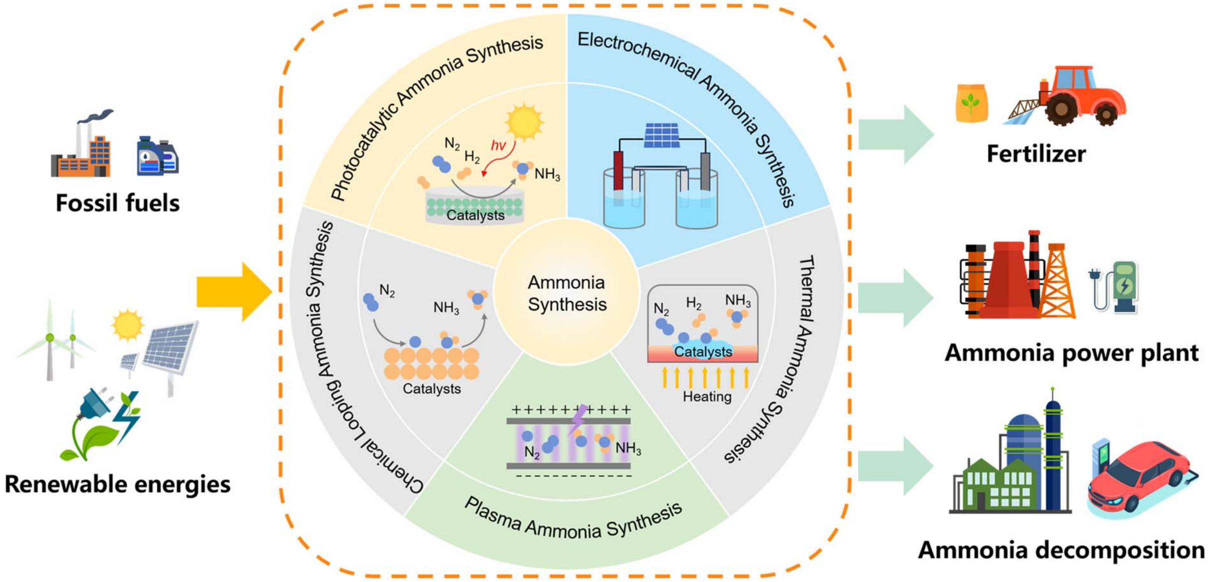

Fig. 1 Pathways for ammonia production and utilization in the energy sector.

a solubility of approximately 35 wt%, which means it can be stably stored in cylinders. Storing ammonia as a solid meets commercial transport conditions and safety standards. Gaseous ammonia is typically stored under low temperature and high pressure in compressed gas cylinders or gas-storage tanks. However, during gaseous storage, it is crucial to tightly regulate the pressure and temperature of the containers to ensure safety and stability.

An efficient transport method is essential for reducing costs, improving transport efficiency, and ensuring safety. Since ammonia is gaseous under standard conditions, it requires liquefaction or high-pressure technology to convert it into liquid or compressed gas for transportation. Liquid ammonia is usually transported using high-pressure containers or specialized storage tanks, while gaseous ammonia can be delivered through compressed gas cylinders or pipelines. Transporting liquid ammonia tends to be more costly but reduces losses and risks during transport, whereas gaseous ammonia is more suitable for short-distance transport, with lower costs but requiring more frequent loading and unloading. The challenges of transporting ammonia involve considerations of the technology, economics, convenience, and practicality. In practice, various factors must be weighed to choose the most suitable transport method, optimizing efficiency, lowering costs, and ensuring safety. Future research should explore new technologies to drive continuous development and innovation in ammonia transport.

2.3 Safety and environmental impact of ammonia

Ammonia is toxic and can irritate or corrode skin and mucous membranes. Exposure to ammonia vapor at concentrations of 1700 ppm can cause lung damage or respiratory failure, while concentrations of 5000 ppm can be fatal. As a result, the use of ammonia is regulated by safety standards. Additionally, due to its pungent odor, ammonia leaks can be detected at concentrations as low as 17 ppm.[11] Ammonia leaks or emissions during production and transport can lead to severe environmental contamination. Once released, ammonia can react with organic compounds in water, forming amine compounds that can cause eutrophication, damage ecosystems, and harm aquatic organisms and plants. To manage ammonia's safety risks effectively, strict safety measures must be implemented, including comprehensive operating procedures, necessary personal protective equipment (such as respirators and protective clothing), leak monitoring systems, and emergency response plans to minimize accident risks and damage.

3 Methods of ammonia production

3.1 Traditional ammonia synthesis methods (Haber–Bosch process)

In the early 20th century, Fritz Haber and Carl Bosch developed the Haber–Bosch process, widely regarded as one of the greatest technological inventions in human history.[12] To date, this process is responsible for producing more than 90% of the world's ammonia. This technology has significantly boosted agricultural production, enabling humanity to produce ample food despite limited land resources. Since its invention, global food production has increased by 7.8 times, while the world population has grown by 4.2 times. The reaction process is as follows:

$$N_2 + 3H_2 \rightarrow 2NH_3,\ \Delta H_{298K} = -92\ \text{kJ mol}^{-1}$$

The nitrogen in syngas is primarily derived from air, while the hydrogen is supplied by fossil fuels, such as coal, oil, and natural gas.[13] Steam methane reforming (SMR) is the most cost-effective industrial method for providing hydrogen for ammonia synthesis.[14,15] Over the past century, catalytic ammonia synthesis has seen tremendous advancements. The production capacity of single ammonia units has increased from 5 tons per day to 2200 tons per day. Energy consumption has dropped from 78 GJ to 27.2 GJ, approaching the theoretical minimum of 20.1 GJ.[16] However, the Haber–Bosch process operates under harsh conditions, typically requiring high temperatures (400–500 °C) and high pressures (10–30 MPa), making it suitable only for large-scale production. Ammonia synthesis is an energy-intensive process, consuming approximately 1.8% of global energy annually and producing 500 million tons of carbon emissions.[12] This massive energy consumption and CO_2 emissions exacerbate global warming, posing severe environmental challenges that conflict with the goals of sustainable development. Therefore, exploring clean energy technologies is crucial for reducing the environmental impact of ammonia synthesis and advancing carbon neutrality and peak carbon strategies.

To enhance energy efficiency and economic viability, it is essential to develop novel ammonia synthesis catalysts that operate under milder conditions. In addition, to eliminate carbon emissions, hydrogen derived from renewable energy sources, such as water electrolysis, should be used as a feedstock. To minimize energy costs, the development of highly active and stable catalysts that function at low temperatures and pressures, along with efficient ammonia separation methods, is necessary. In this section, we focus on the latest advancements and challenges in ammonia-synthesis catalysts and discuss alternative methods to the Haber–Bosch process, including chemical looping, electrocatalysis, photocatalysis, and plasma catalysis.

3.2 Renewable-energy-driven ammonia-synthesis technologies

3.2.1 Thermal ammonia-synthesis catalysis. It is well known that the adsorption and activation of nitrogen (N_2) molecules at active sites are critical initial steps in ammonia synthesis. A nitrogen molecule consists of two linearly bonded nitrogen atoms, each with a pair of electrons in the 2s orbital with opposite spins, and three lone electron pairs in the 2p orbitals with the same spin (Fig. 2). Upon orbital hybridization, bonding (σ and π) and antibonding (σ* and π*) orbitals are formed. The electrons in the π and 2σ orbitals generate a highly stable triple bond (N≡N). As a result, the inert nature of nitrogen makes its reduction under mild conditions particularly challenging. The main difficulties include:

(1) The N_2 molecule has a very high bond dissociation energy of 941 kJ mol^{-1}, requiring significant energy to break the N≡N triple bond. Thus, the dissociation of N_2 is often regarded as the rate-determining step in ammonia synthesis; (2) N_2 has a negative electron affinity (−1.9 eV) and a high ionization energy (15.85 eV), resulting in low reactivity; (3) from a kinetic perspective, the large energy gap (~10.82 eV) between the highest occupied molecular orbital (HOMO) and the lowest unoccupied molecular orbital (LUMO) further impedes electron transfer;[18,19] (4) the first hydrogenation step of the N_2 molecule is an endothermic reaction ($\Delta H = 37.6$ kJ mol^{-1}), making the protonation process thermodynamically unfavorable.

Previous studies have shown that transition metals (TMs) can activate N_2 by forming N–metal bonds.[20,21] Here, the vacant d-orbitals of TM atoms accept the lone pair of electrons from N_2, while the delocalized electrons of the TM are simultaneously transferred to the N_2 antibonding (π*) orbitals through a back-donation mechanism, thereby weakening the N≡N triple bond.[22] However, the linear scaling relationship in ammonia synthesis makes it difficult to enhance both the N_2 activation and ammonia-production rates simultaneously. As a result, catalyst design requires a trade-off approach, where the optimal ammonia-synthesis catalyst must have a nitrogen adsorption strength that is neither too strong nor too weak. Fig. 3a and b illustrate the impact of the linear scaling relationship on catalytic ammonia synthesis over transition metal surfaces.[17] The ammonia-synthesis activity of transition metals follows a typical "volcano plot" pattern, as shown in Fig. 3c. Iron (Fe) and ruthenium (Ru) are located near the peak of this curve, exhibiting a balanced nitrogen binding strength and high catalytic activity for ammonia synthesis. Studies suggest that combining metals from both sides of the volcano plot may optimize nitrogen binding. For instance, Co–Mo catalysts have achieved ammonia synthesis activity comparable to Ru-based

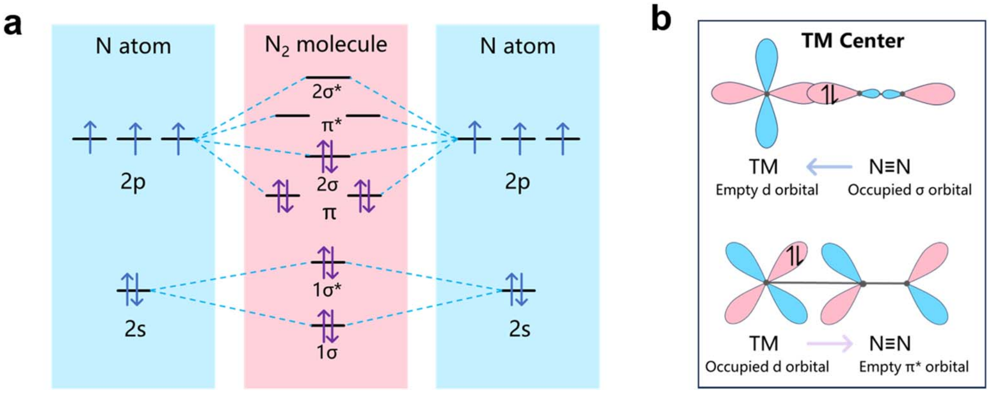

Fig. 2 (a) Schematics of N atomic orbitals and N_2 molecular orbitals. (b) Simplified schematic of N_2 bonding to TMs.

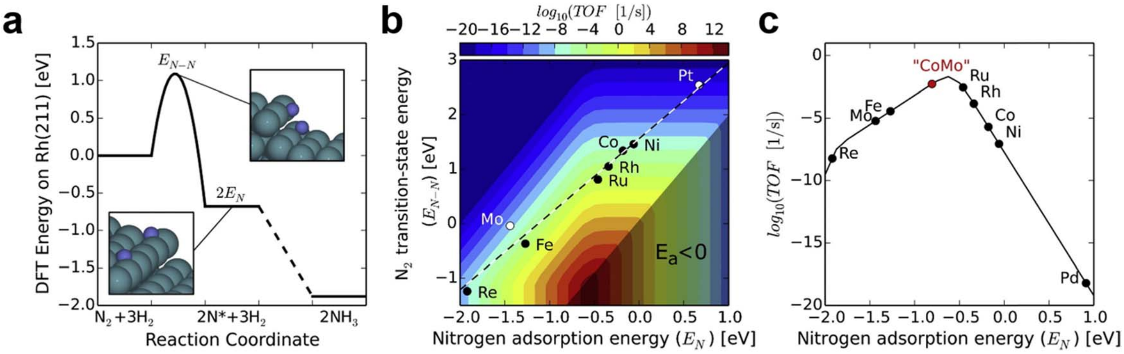

Fig. 3 (a) Potential energy diagram for a simplified ammonia synthesis reaction. (b) Ammonia synthesis rate as a function of nitrogen adsorption energy and the N_2 dissociation barrier with energetics for stepped transition metal sites (c) calculated rate as a function of a single descriptor of E_N.[17] Copyright 2015, reproduced with permission from Elsevier.

catalysts. The success of this catalyst design strategy demonstrates that rational catalyst design can break the linear scaling relationship in ammonia synthesis. Breaking this relationship is key to improving the reaction kinetics and achieving low-energy operating conditions.[1,23]

Consequently, many researchers have focused on breaking the linear scaling relationship in ammonia synthesis. Chen *et al.* introduced a dual-active-center system by incorporating LiH as a secondary component into a supported transition metal catalyst (TM-LiH), which demonstrated significantly enhanced ammonia synthesis performance under mild conditions.[24] Here, N_2 molecules dissociate on the transition metal surface to form TM–N. The nitrogen atom then migrates to LiH, forming Li–N–H species, which subsequently undergoes stepwise hydrogenation to produce NH_3, eventually desorbing from the catalyst surface (Fig. 4a). The construction of dual-active centers allows for the activation of N_2 and H_2, as well as the adsorption of intermediate species, to occur at different active sites, thereby overcoming the limitation between the reaction barriers and adsorption energies. Hosono *et al.* developed a "dual-active-site" catalyst by loading nickel nanoparticles onto lanthanum nitride (LaN) crystals, achieving stable and efficient ammonia synthesis.[25] In this system, H_2 and N_2 are activated at spatially separated sites: H_2 by the nickel metal supported on LaN and N_2 by the Mars–van Krevelen mechanism, where nitrogen vacancies on LaN bind and activate N_2 (Fig. 4b). By using distinct sites for activating the reactants and leveraging the synergistic effects, this new catalyst exhibited activity surpassing that of traditional cobalt- and nickel-based catalysts, and comparable to ruthenium-based systems. Subsequent studies synthesized several new materials, such as Co/SrNH,[29] La_3AlN,[30] and Co/CeN,[31] which all demonstrated excellent ammonia synthesis performance.

Zhang *et al.* explored an alternative to the widely accepted strong–weak nitrogen adsorption pair in ammonia synthesis. They discovered that the bifunctional nanocatalyst $TiO_{2-x}H_y$/Fe exhibited higher activity than Fe alone, despite $TiO_{2-x}H_y$ having stronger nitrogen adsorption (−1.95 eV *vs.* −1.59 eV).[26] This revealed a new strong–strong nitrogen adsorption pair. N_2 and H_2 dissociate on Fe, while the unique O_V–H structure of $TiO_{2-x}H_y$ facilitates hydrogen spillover at O_V sites, promoting easier hydrogenation reactions at these active centers (Fig. 4c). This study simultaneously reduced the reaction barriers for N_2 dissociation and nitrogen hydrogenation using bifunctional active sites. Gao *et al.* designed lithium-intercalated MoO_{2-x} nanosheets with Mo and Fe dual-active sites. Mo(III) primarily activates N_2, while Fe facilitates H_2 activation and NH_x formation, leading to efficient and stable ammonia synthesis.[32] The insertion of Li^+ and the balanced electron flow shifts the d-band center of MoO_{2-x} downward, significantly lowering the E_N and promoting the conversion of NH_x intermediates at lower temperatures, thus enhancing ammonia synthesis.

Another approach to enhancing ammonia synthesis catalysts involves introducing electronic or structural promoters, which increase the electron-donating capacity of transition metals, thereby facilitating N_2 dissociation and enabling ammonia synthesis under mild conditions.[33–35] Inorganic electrides, which possess cavities filled with abundant electrons, are materials characterized by a low work function and high electron density.[36] Hosono reported a series of inorganic electrides, such as C12A7:e^-,[27] Ca_2N:e^-,[37] Y_5Si_3,[38] and LaRuSi,[39] which, when used as supports for transition metal catalysts, could donate more electrons to Ru, thereby accelerating the ammonia synthesis reaction. C12A7:e^- is considered the first stable electride compound at room temperature, with excellent conductivity, abundant charge carriers, and a low work function (2.4 eV), as shown in Fig. 4d. On Ru/C12A7:e^- catalysts, the dissociative adsorption rate of N_2 was significantly enhanced, with the activation energy for this step dropping from 104 kJ mol^{-1} to below 29 kJ mol^{-1}. The rate-determining step of the reaction shifted from N_2 dissociation to NH_x formation. As research into these materials progresses, the theoretical basis for their catalytic activity in ammonia synthesis is being further refined and validated.

Recent studies have proposed a spin-mediated mechanism for promoting ammonia synthesis by introducing heterometal atoms at the catalyst's active sites, which can activate traditionally inert magnetic materials, such as cobalt (Co), for ammonia synthesis. Ib Chorkendorff, Jens K. Nørskov, and others combined DFT calculations with experiments to verify

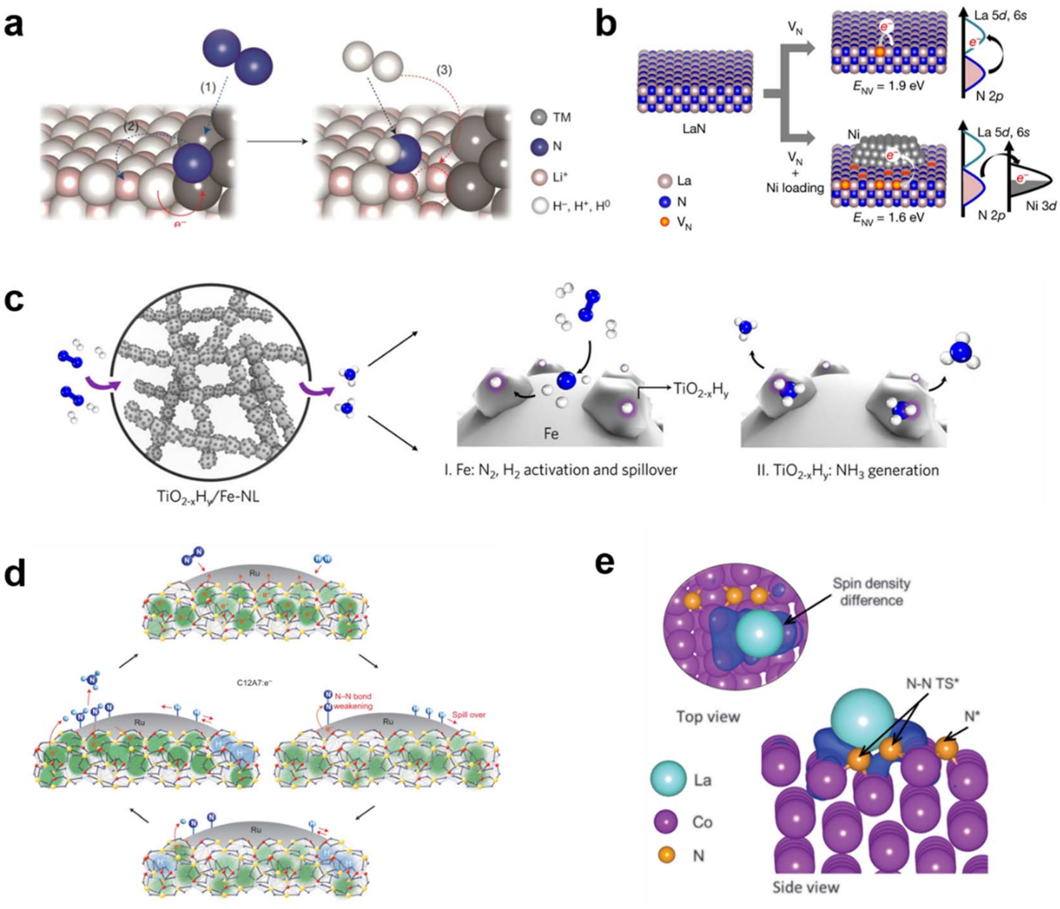

Fig. 4 (a) Schematic of the mechanism of LiH as a dual-active center.[24] Copyright 2017. Reproduced with permission from Springer Nature. (b) Schematic of the formation of nitrogen vacancies (V_N) and the related electron-transfer pathways.[25] Copyright 2020. Reproduced with permission from Springer Nature. (c) Schematic of N_2 and H_2 activation on Fe and transfer to $TiO_{2-x}H_y$ for NH_3 generation over the $TiO_{2-x}H_y$/Fe catalyst.[26] Copyright 2020, reproduced with permission from American Chemical Society. (d) Possible pathway for the ammonia synthesis reaction over Ru/C12A7:e$^-$.[27] Copyright 2012, reproduced with permission from Springer Nature. (e) Spin density difference at the adsorption site of N* and N–N transition state on La-promoted Co.[28] Reproduced with permission from AAAS.

the spin-mediated promotion mechanism in the La/Co system, as illustrated in Fig. 4e. By studying Co single crystals and Co nanoparticles under ambient pressure, they identified the active site for ammonia synthesis as the B5 site on Co adsorbed with La. Under the conditions of 350 °C and 1 bar, the La/Co system demonstrated higher catalytic activity than other model catalysts tested under the same conditions.[28] It is important to note that Co is typically quite inert toward N_2 dissociation, even with alkali metal promotion, showing only marginal ammonia synthesis activity. Given the significant role of electrostatic effects in explaining the promotion by Cs and K, the research team suggested that this effect could also account for the extraordinary promotion of Co by Li, Ba, Ca, and La. However, the additional promotion of Co by Li, Ba, Ca, and La was found to be related to Co's spin polarization. These unconventional promoters reduce the spin polarization of neighboring Co atoms, thereby facilitating N_2 dissociation. This additional promotion effect is proportional to the reduction in the spin magnetic moments of Co atoms induced by the magnetic cocatalysts. Thanks to this anomalous spin-promotion effect, these promoters can minimize the spin moments of metal atoms, thereby lowering the transition state energy barrier for N_2 dissociation, ultimately enhancing catalytic efficiency.[40] Additionally, Wang *et al.* used DFT calculations to reveal the impact of ferromagnetic-to-paramagnetic phase transitions on the catalytic performance of ferromagnetic metals. They proposed a strategy to drive cobalt and nickel toward the Sabatier peak for ammonia synthesis through this phase transition, offering valuable insights for designing high-performance catalysts in the future.[41]

3.2.2 Chemical looping ammonia synthesis (CLAS). Chemical looping ammonia synthesis (CLAS) can break the linear scaling relationship by decomposing the ammonia synthesis reaction into several sub-reactions.[42] Thus, N_2 dissociation and the desorption of nitrogen-containing intermediates can occur at different reaction sites. By using redox catalysts to mediate ammonia synthesis in a stepwise reaction, CLAS avoids the competitive adsorption of N_2 and H_2 on metal catalysts, as well as the conflict between the kinetics and thermodynamics in the Haber–Bosch process.[42,43]

The CLAS process involves ammonia synthesis reactions taking place in two interconnected reactors: an ammoniation reactor and a nitridation reactor. In the ammoniation reactor, nitrogen-containing intermediates donate their lattice N atoms to H_2 or H_2O, producing NH_3 through hydrogenation or hydrolysis. In the nitridation reactor, the de-nitrogenated intermediates are regenerated by reaction with nitrogen gas. Common CLAS processes can be represented by four schemes, as shown in Fig. 5, and can be divided into two categories: ammonia synthesis using H_2O as the hydrogen source (H_2O-CLAS) and ammonia synthesis using H_2 (H_2-CLAS).[44] The latter, depending on the type of nitrogen carrier, can be further divided into alkali metal hydride/alkaline earth metal hydride-mediated AH-CLAS and metal nitride-mediated MN-CLAS.

In the H_2O-CLAS process, transition metals act as electron donors for N_2 activation, and since water is used as the hydrogen source, no additional large-scale hydrogen-production steps are needed, thereby reducing the dependence on fossil fuels. However, the main drawbacks of this process are the high reduction temperature of metal oxides (around 1000 °C) and the need for additional reducing agents. In recent research by Abanades *et al.*, experiments were conducted to screen potential metal nitrides for use in the solar thermochemical H_2O-CLAS process. The catalytic process flowchart is shown in Fig. 6a, and the results indicated that FeN, CrN, BN, and Si_3N_4 exhibited low NH_3 yield at 1000 °C, while AlN, Li_3N, Ca_3N_2, Mg_3N_2, TiN, and ZrN demonstrated temperature-dependent reactivity.[45]

Metal nitrides were among the first redox catalysts used in H_2-CLAS. MN-CL is very similar to H_2O-CL, as it also uses metals as electron donors for N_2 activation. In MN-CL, the metals are nitrided in a nitrogen stream and then reduced to their metallic state by hydrogen, producing ammonia. This process occurs under relatively mild conditions (1 bar, <800 °C), and the reaction system and operation are relatively simple, without requiring sacrificial reducing agents.[48] However, the ammonia-production rate is low, limiting its industrial applicability. Typically, single metal nitrides are often too stable to be reduced by hydrogen under mild conditions to produce ammonia, or the reduced samples exhibit slow ammonia-production rates. Therefore, composite materials combining two or more metals with ideal catalytic properties have been widely studied. Hargreaves *et al.* prepared alkali metal or transition metal ion-doped Mn_3N_2 (A–Mn–N, A = Fe, Co, K, Li) and investigated the effect of the chemical composition on the reactivity of the lattice nitrogen. The results showed that the mobility of lattice nitrogen was improved across all the A–Mn–N systems studied.[49] However, only Li–Mn–N exhibited high reactivity, as its hydrogenation step proceeded significantly faster. To further elucidate the effect of lithium doping on the H_2-CLAS reaction, they combined N_2/H_2 isotope exchange reactions with DFT theoretical calculations. The results indicated that lithium doping reduced the nitrogen vacancy formation energy and increased the proportion of the θ-Mn_6N_{5+x} phase, thereby enhancing the lattice nitrogen reactivity.[50]

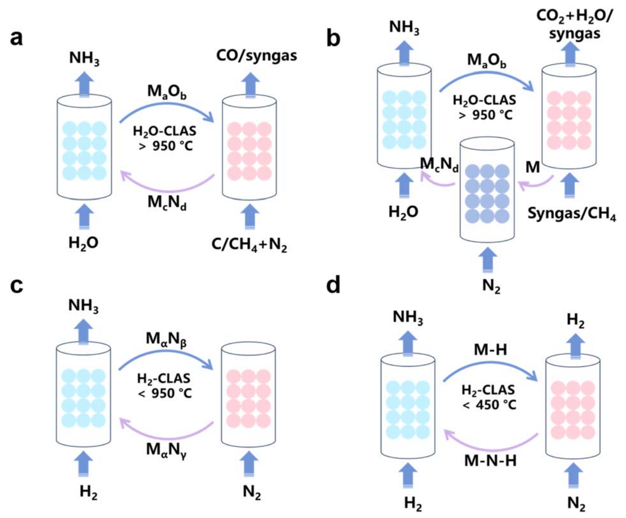

Fig. 5 Schematic of the typical chemical looping ammonia synthesis processes. (a) Two-step H_2O-CLAS process mediated by M_cN_d/M_aO_b redox pairs; (b) three-step H_2O-CLAS process mediated by $M/M_cN_d/M_aO_b$ redox pairs; (c) H_2-CLAS process mediated by $M_\alpha N_\beta/M_\alpha N_\gamma$ redox pairs; (d) H_2-CLAS process mediated by metal hydride (M–H)/metal nitride-hydride (M–N–H) redox pairs.

Metal nitride composites with specific crystal structures and fixed compositions are often used in various redox cycling reactions due to their excellent structure, reversible redox properties, and the synergy between different cations.[51] Binary metal composites (Fig. 6b), such as Mn–Fe-based nitrides,[52,53] Li–Sn alloy,[54] anti-perovskite nitrides,[46] and Co–Mo–N systems,[55] have been applied in H_2-CLAS reactions. Goto *et al.* conducted a series of studies on anti-perovskite nitrides (Co_3ZnN, Ni_3ZnN, Co_3InN, and Ni_3InN) in H_2-CLAS reactions. The Ni-nitrides exhibited excellent performance, and the intermediates Ni_3ZnN_x and Ni_3InN_y were detected during the reaction.[46] From a thermodynamic perspective, the smaller the energy gap between the nitridation and denitrification steps, the more favorable the H_2-CLAS process, as shown in Fig. 6c.[42] Alkali metal/alkaline earth metal hydrides can also serve as nitrogen carriers in CLAS. The typical AH-CL process consists of two steps: (1) N_2 is reduced by AH to form metal imide (ANH); (2) ANH is hydrogenated to produce ammonia and regenerate AH. AH-CL synthesizes ammonia using H_2 and N_2 as feedstocks, with the hydride ions in metal hydrides serving as hydrogen donors and electron donors with a high N_2-reduction activity, allowing nitrogenation to occur at relatively low temperatures.[47,56] Gao *et al.* proposed a low-temperature chemical looping ammonia synthesis technology using alkali (earth) metal imide compounds as nitrogen carriers. In this process, the hydrides of alkali (earth) metals first "fix" nitrogen to form the corresponding imide compounds, and then the atmosphere is switched to hydrogen to hydrogenate the imide compounds, releasing ammonia. The process flowchart is shown in Fig. 6d, in which it can be seen that the Li–N–H and Ba–N–H systems exhibited moderate thermodynamics for nitrogenation and hydrogenation. With the assistance of transition metal catalysts, ammonia synthesis could be achieved at ambient pressure and 100 °C.[47] At 250 °C, the ammonia-production rate of this

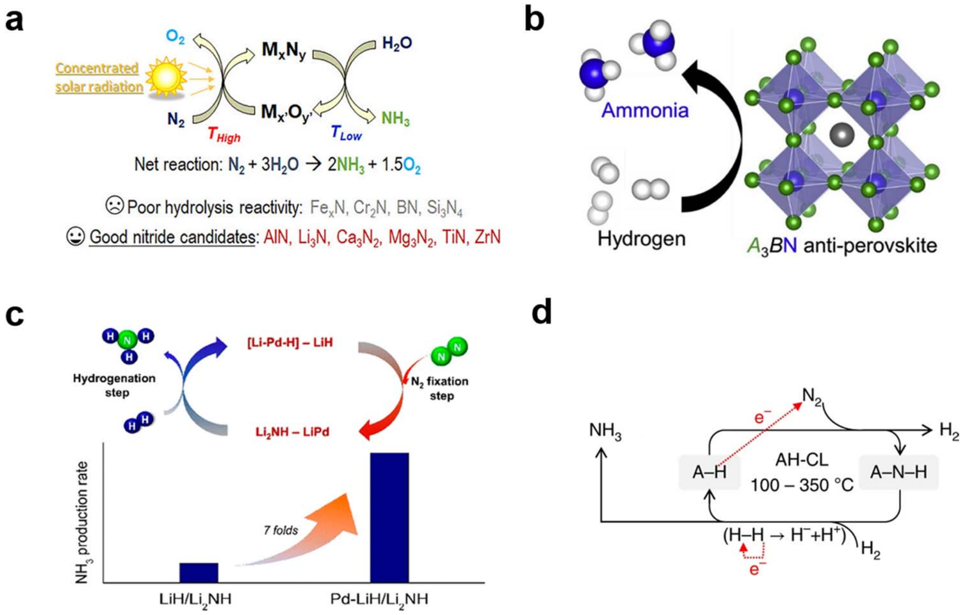

Fig. 6 (a) Reaction process of solar-driven chemical looping.[45] Copyright 2024, reproduced with permission from Elsevier. (b) $A_xB_yN_z$ complex nitride redox catalysts for H_2-CLAS.[46] Copyright 2021, reproduced with permission from Elsevier. (c) NH_3 production rate of the Pd-modified LiH/Li_2NH pair in the H_2-CLAS process.[42] Copyright 2024, reproduced with permission from Elsevier. (d) Reaction process of AH-CLAS, A = Ba, Li.[47] Copyright 2018, reproduced with permission from Springer Nature.

process was about an order of magnitude higher than that of the highly active Cs–Ru/MgO catalytic process. AH-CL exhibited faster reaction kinetics and a higher NH_3 yield due to the good synergy between alkali/alkaline earth metal hydrides and transition metal nitrides.

However, the chemical and thermal stability of the reactants were poor. CLAS is a rapidly developing research field with promising prospects and applications. To achieve carbon peak and carbon neutrality goals, CLAS should advance toward lowering the reaction temperatures, improving the reaction kinetics, and utilizing renewable energy sources.

3.2.3 Plasma ammonia synthesis. Plasma-assisted ammonia synthesis technology has garnered significant attention for its ability to efficiently synthesize ammonia under mild conditions. This technology uses high-energy electric fields to induce vibrational excitation and the ionization of gas molecules, thereby promoting molecular reactions.[59] This technology operates under lower temperature and pressure conditions and is suitable for small-scale and distributed ammonia synthesis systems. Moreover, while plasma technology typically relies on electrical energy, the plasma ammonia synthesis process is compatible with intermittent renewable energy sources (such as solar and wind), offering potential applications in energy diversification and sustainable development.

The concept of plasma was first introduced by physicist William Crookes in the 1860s.[60] Plasma, the fourth state of matter, is composed of electrons, various ions, molecules, and their free radicals and excited states. The introduction of plasma can promote the activation of N_2 molecules, with plasma-induced vibrational excitation significantly lowering the dissociation barrier of N_2 molecules, as shown in Fig. 7a.[57] Mehta *et al.* developed a microkinetic model based on density functional theory to account for this effect, and parameterized the model using the vibrational excitation of N_2 observed in dielectric barrier discharge plasma. Fig. 7b shows a plasma volcano plot, revealing that the introduction of plasma shifts the volcano peak to the right, toward metals with weaker nitrogen binding energy, predicting Co and Ni to be near the volcano peak.[57] The rate enhancement occurs only when N_2 dissociation is rate-limiting, as metals with weaker nitrogen binding energies have lower hydrogenation barriers, resulting in a greater rate enhancement. The ammonia-synthesis rates observed in dielectric barrier discharge plasma reactors align with the predicted enhancements in optimal metal catalysts, providing guidance for designing plasma catalysts. Engelmann *et al.* studied how plasma-generated free radicals and vibrationally excited N_2 interact with catalysts and affect the NH_3 turnover frequency (TOF).[58] In the presence of free radicals in the plasma phase, the process follows a surface-enhanced plasma-driven synthesis, meaning free radicals are the primary source of N and H. Under these conditions, it was found that free radical adsorption reactions largely eliminate the dependence on the catalyst binding energy, as shown in Fig. 7c. Additionally, the Eley–Rideal reaction significantly reduces reliance on the catalyst binding energy. In this way, reactions involving plasma-generated free radicals contrast with the volcano behavior under thermal conditions or plasma conditions involving only vibrational excitation. In summary, the proportion of N, H, and NH_x radicals depends on the specific energy input (SEI). In turn, the density of these plasma-generated radicals seems to determine whether the Langmuir–

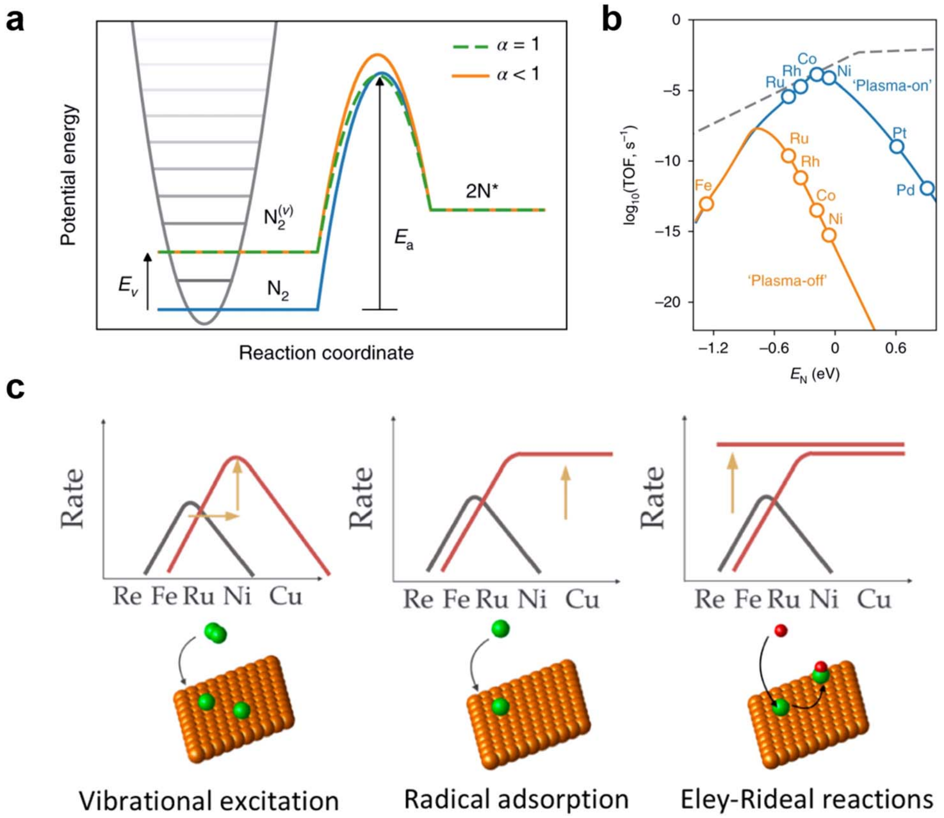

Fig. 7 (a) Reaction coordinate diagram comparing the activation energies for N_2 dissociation starting from the ground (blue) or second vibrationally excited states.[57] Copyright 2018, reproduced with permission from Springer Nature. (b) Comparison of N_2 vibrational-distribution-weighted (plasma-on) and thermal (plasma-off) ammonia-synthesis rates.[57] Copyright 2018, reproduced with permission from Springer Nature. (c) Proposed model for elucidating the trends and concepts of catalytic reactions under the presence of free radicals.[58] Copyright 2021, reproduced with permission from American Chemical Society.

Hinshelwood mechanism, Eley–Rideal reaction, or plasma-phase reactions dominate.[61]

The interaction mechanism between plasma and catalysts is highly complex. The plasma environment contains various species, including electrons, positive and negative ions, photons, free radicals, and neutral atoms and molecules in their ground or vibrationally excited states. These species can interact with catalysts in several ways: (1) altering the plasma characteristics, (2) initiating new reaction pathways through radical reactions in the plasma environment, and (3) through the surface reactions of plasma active species on the catalyst surface. Exploring the interactions between catalysts and plasma requires multidisciplinary approaches, and most information is currently obtained through macroscopic performance tests of plasma reactors. The effects of different catalysts on N_2 and H_2 plasma ammonia synthesis are shown in Table 1.

The first mechanism, altering plasma characteristics, may affect the discharge conditions within the plasma reactor when dielectric material fillers are used. For example, the enhancement of the electric field may lower the plasma initiation voltage, and the increased electric field can raise the electron temperature, leading to stronger electron impact reactions in the system, thereby influencing plasma chemistry. High dielectric constant materials have been shown to significantly enhance catalytic activity in plasma ammonia synthesis in existing studies.[64,77,78] Akay *et al.* used high-dielectric-constant barium titanate spheres as fillers to investigate the effect of the dielectric constant on plasma reactions. They found that materials with high dielectric constants could promote the plasma electric-field strength, generating more active species, facilitating reactions, and reducing the energy consumption of dielectric barrier discharge (DBD) ammonia synthesis from nitrogen and hydrogen at low temperature and atmospheric pressure. They termed these high dielectric constant spheres "Plasma Catalysis Promoters" (PCPs).[63]

Navascués *et al.* used a ferroelectric material, namely pellets of lead zirconate titanate (PZT), as fillers to enhance the plasma discharge intensity. Ferroelectric packed-bed reactors, using high-dielectric-constant PZT materials, exhibited a high plasma current.[79] Additionally, the filler materials promoted the formation of microdischarges, and the discharges could even shift entirely from the gas phase to the catalyst surface. Shah *et al.* used zeolite 5A in DBD plasma ammonia synthesis, where the presence of zeolites promoted the formation of microdischarges, altering the reactor's voltage–current characteristics, thereby improving the catalytic performance. The disturbance of the electronic properties on the zeolite surface by

Table 1 Effect of plasma combined with different catalysts for the synthesis of ammonia from N_2 and H_2

Discharge type	Catalyst	NH_3-production rate (μmol g^{-1} h^{-1})	Energy yield (g_{NH_3} kW^{-1} h^{-1})	Energy cost (MJ mol^{-1})	Ref.
Haber–Bosch		—	—	0.49	62
DBD	Ni/SiO_2–$BaTiO_2$	502	0.57	81	63
DBD	PZT	—	0.45	68	64
DBD	Au-wool	73	—	—	65
RF	Ga	—	0.22	278.18	66
RF	Ga–In	—	0.31	196	67
DBD	$RuMg/\gamma$-Al_2O_3	565	25.5	—	68
DBD	CoNi–Al_2O_3	1500	—	73.73	69
DBD	MgO	—	0.94	—	70
DBD	Ru–carbon	—	0.66	—	71
DBD	Ni–Al_2O_3	471	0.29	437.14	72
DBD	Zeolite 5A	930	15.5	3.99	73
DBD	ZIF-8, ZIF-67	2530	—	—	74
DBD	Ni–Mg/SBA-15	—	1.05	—	75
DBD	Ni-MCM-41	3959	1.2	40.8	76

atmospheric plasma enhanced the reactive states on the surface, promoting nitrogen dissociation and subsequent ammonia formation.[73]

The second mechanism involves utilizing plasma radicals in reactions. Surface reactions can strongly affect the main reaction pathways, influencing the product distribution.[83] When surface reactions tend to generate products rather than recombination reactions, the reaction yield is significantly enhanced, which is unachievable in thermal catalysis. It is also worth noting that radicals and ions in the plasma may react with other surface species, formed through the dissociative adsorption of non-activated molecules. Rouwenhorst *et al.* discussed plasma-enhanced catalysis for ammonia synthesis at temperatures between 473–603 K, based on kinetic data. They compared the activation energies of thermal catalysis and plasma-enhanced catalysis. In both processes, the influence of promoters and supports on the activity was similar, as shown in Fig. 8a, indicating that the catalyst's ability to dissociate N_2 remained crucial, even under plasma conditions.[80] Engelmann *et al.* developed a microkinetic model for plasma-catalyzed ammonia synthesis, including plasma-generated N atoms, NH_x radicals, and vibrationally excited N_2.[58] Based on various model DFT calculations and experimental data, it was concluded that N_2 dissociation was no longer the rate-determining step in ammonia synthesis, with surface hydrogenation becoming the rate-determining step in plasma-driven ammonia synthesis. Shah *et al.* combined theoretical calculations and experiments, suggesting that the hydrogenation step mainly follows the Langmuir–Hinshelwood mechanism on Fe catalysts, while the contribution from the Eley–Rideal (E–R) mechanism may increase with higher plasma power and pressure.[66] Hong *et al.* also studied plasma-catalyzed ammonia synthesis under different plasma states. They concluded that mechanistically, these pathways are determined by the large number of hydrogen atoms adsorbed on the surface, and proposed that the E–R reaction is essential in plasma catalysis.[60] Wu *et al.* proposed and developed a plasma-driven, two-step chemical looping ammonia synthesis process mediated by alkali metal hydrides, such as sodium hydride (NaH), as shown in Fig. 8b. NaH cannot fix nitrogen under thermal chemical conditions, but the introduction of plasma facilitates nitrogen fixation by NaH, producing nitrogen-containing products such as $NaNH_2$. Based on power and temperature measurements, the authors speculated that H_2 primarily originates from the redox reactions between N_2 and H^-.[81] Based on experimental data analysis, two possible reaction pathways for $NaNH_2$ formation were proposed. One pathway involves redox reactions between the active N_2 or N species generated by plasma and NaH, forming N–H bonds and H_2. Another pathway might involve NaH decomposition under plasma conditions, generating unsaturated NaH_{1-x} and H_2, followed by gas-phase reactions between H_2 and N_2 to form NH_3, which then reacts with NaH to produce $NaNH_2$. In summary, the fractions of N, H, and NH_x radicals depend on the specific energy input (SEI). In turn, the density of these plasma-generated radicals appears to determine whether the Langmuir–Hinshelwood mechanism, Eley–Rideal reaction, or even plasma-phase reactions dominate.

A third mechanism involves the surface reactions of plasma-activated species. The prerequisite for effective interaction between plasma and catalyst is that the plasma-activated species reach the catalyst surface before recombining or decaying into ground-state molecules. The diffusion distance before recombination into neutral molecules or decay to the ground state is limited, so the interaction between plasma and the catalyst surface only occurs when the distance between them is smaller than the maximum travel distance of the plasma-activated species. When the catalyst is a porous material, plasma can be generated inside large pores, provided that the pore size is greater than the Debye length.[84] Theoretical simulations have concluded that plasma can be generated inside pores larger than 10 μm. Thus, only plasma-activated species with sufficiently long lifetimes can penetrate the pores, while most other species will recombine or decay to their ground states before reaching the active catalyst surface within the pores. As a result, in most cases, the contribution from the external surface area may dominate. Wang *et al.* proposed

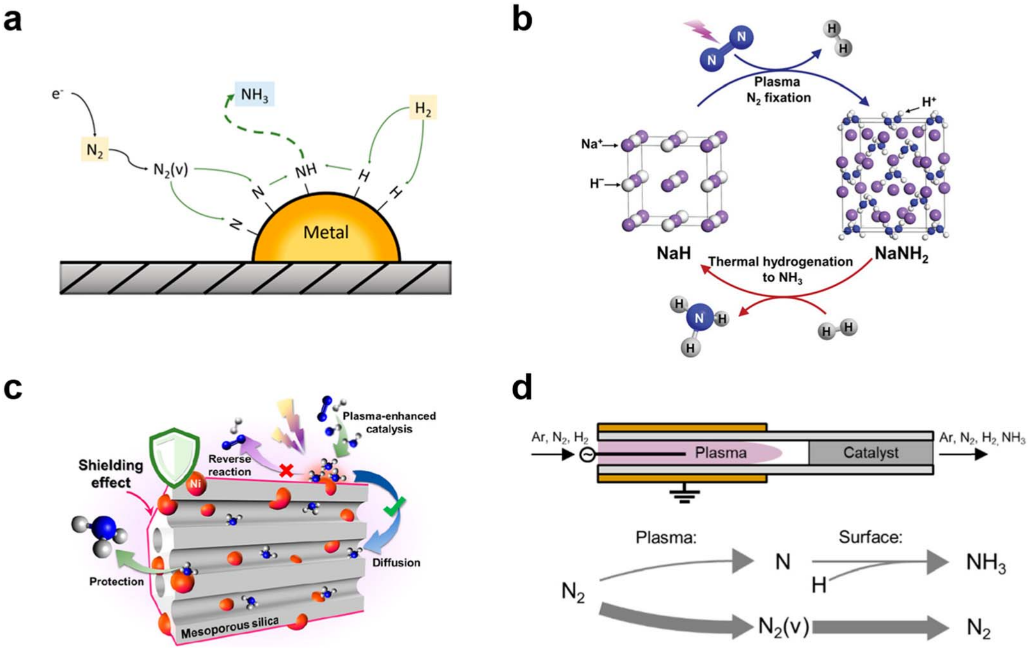

Fig. 8 (a) Reaction mechanisms of plasma-enhanced catalytic ammonia synthesis.[80] Copyright 2019, reproduced with permission from American Chemical Society. (b) Conceptual cycle for plasma-driven chemical looping ammonia synthesis (PCLAS) mediated by the interconversion of NaH and $NaNH_2$.[81] Copyright 2023, reproduced with permission from Wiley-VCH. (c) Schematic of the proposed mechanism for the plasma-assisted surface reaction and the "shielding protection" effect of mesoporous MCM-41.[74] Copyright 2022, reproduced with permission from American Chemical Society. (d) Setup to measure the species densities at the outlet of the packed bed from reactions between Ar/N_2 plasma-derived species and unreacted H_2.[82] Copyright 2023, reproduced with permission from American Chemical Society.

a "shielding protection" catalyst design strategy based on the interaction between plasma and customized mesoporous catalysts, aiming to limit plasma-induced ammonia decomposition during the synthesis of ammonia in dielectric barrier discharge (DBD) reactors. The designed catalyst achieved an NH_3 synthesis rate of 5% at 60 kJ L^{-1} under plasma conditions, the best result among plasma-assisted NH_3 synthesis systems to date. As shown in Fig. 8c, the NH_3-concentration gradient on the mesoporous framework drives the formed NH_3 to diffuse into the mesopores, thereby limiting the plasma-induced reversible reaction (NH_3 decomposition) caused by non-discharge plasma in the mesopores, *i.e.*, providing "shielding protection," shifting the reaction equilibrium toward higher NH_3 production.[76] Bayer *et al.* quantitatively linked the consumption of plasma-derived species [N, H, and N_2(v)] to NH_3 formation by measuring their densities, and monitored the consumption of plasma-derived species at different residence times. This allowed them to elucidate the species, pathways, and the timescales involved in plasma-catalyzed NH_3 formation on transition metals. The consumption of N coincided with NH_3 formation on the same timescale, further confirming that N-related reactions contributed to NH_3 formation.[82]

Future research directions include further optimizing the plasma reaction conditions to improve the ammonia-synthesis efficiency and yield. Additionally, more effective catalysts and reactor designs need to be explored to reduce energy consumption and minimize byproduct formation. A deeper understanding of the role of plasma in ammonia synthesis, through continuous exploration at both the experimental and theoretical levels, would also contribute to the broader application and further development of this technology in industrial settings.

3.2.4 Photocatalytic ammonia synthesis. Photocatalytic ammonia synthesis (PAS) is a process that utilizes solar energy as the primary driving force to convert N_2 into NH_3 under ambient temperature and pressure conditions. This innovative catalytic method has the following key characteristics: (1) environmental friendliness: PAS uses renewable light sources, such as sunlight, to drive the reaction, significantly reducing the reliance on fossil fuels compared to the traditional Haber–Bosch process and decreasing greenhouse gas emissions; (2) low energy consumption: the energy required for photocatalytic processes is typically lower than that of the traditional high-temperature, high-pressure ammonia synthesis, making PAS a potentially more energy-efficient approach. This is crucial for mitigating the energy crisis and achieving carbon neutrality; (3) mild reaction conditions: PAS typically operates under ambient temperature and pressure, reducing operational complexity, equipment costs, and enhancing process safety. In 1977, Schrauzer and Guth first discovered that TiO_2-based photocatalysts could perform ammonia synthesis under UV light, thus pioneering the field of photocatalytic ammonia synthesis.[87] The photocatalyst absorbs sunlight, inducing photoexcitation to generate electrons and holes. The electrons in the conduction band migrate to the catalyst's active sites, where they activate N_2. The holes left in the valence band oxidize H_2O to O_2, releasing the protons required for ammonia synthesis. The activated N_2 reacts with the protons to form NH_3, as illustrated in Fig. 9a.[85] Unlike the dissociative mechanism in the Haber–Bosch process, which requires high temperature to break the N≡N triple bond, PAS operates under mild conditions through a stepwise proton-coupled electron transfer (PCET) mechanism that gradually hydrogenates N_2, as shown in Fig. 9b.[86] Based on the hydrogenation sequence, there are two possible pathways: the distal pathway and the alternating pathway. In the distal pathway, the N atom furthest from the photocatalyst is hydrogenated first to form NH_3, followed by the hydrogenation of the second N atom to form another NH_3 molecule. In the alternating pathway, the two N atoms are hydrogenated alternately, releasing two NH_3 molecules sequentially.

Various photocatalysts for ammonia synthesis have been developed, including metal oxides, metal sulfides, graphitic carbon nitride (g-C_3N_4), layered double hydroxides (LDHs), and organic frameworks (metal–organic frameworks (MOFs) and covalent organic frameworks (COFs)). An ideal photocatalyst should exhibit strong visible-light absorption, a high carrier-separation efficiency, robust stability, large surface area, and tunable structure. Designing well-constructed active sites with a strong electron-donating capability and controlling the photo-induced electron-transfer process are key to achieving efficient photocatalytic N_2 activation. TiO_2 is an excellent photocatalyst for ammonia synthesis. Zhang *et al.* constructed continuously tunable oxygen vacancies on TiO_2, achieving a high ammonia yield of 324.86 μmol h^{-1} g^{-1} at 340 °C, which was 3.85 times that of the pristine TiO_2. The improved catalytic efficiency was attributed to the presence of oxygen vacancies in the photocatalyst, which enhanced nitrogen adsorption and activation, as well as the charge-separation efficiency.[92] Fu *et al.* achieved the surface metallization of TiO_2 semiconductor materials through surface F^--ion doping. The strong electronic repulsion between F^- and adjacent Ti^{3+} resulted in F–TiO_{2-x} having a lower work function and better electron-donating ability. By introducing Ru metal nanoclusters as active sites on the surface, the efficient activation of nitrogen molecules was achieved due to ohmic contact at the metal–semiconductor interface, which facilitated the transfer of photogenerated electrons from the catalyst to the Ru active sites, as shown in Fig. 10a. Furthermore, the metallized surface and abundant bulk Ti^{3+} could effectively absorb photons in the infrared spectrum, enabling the material to exhibit excellent photocatalytic ammonia-synthesis activity across the visible and near-infrared regions (400–1550 nm).[88] Liu *et al.* designed a B-doped TiO_2 photocatalyst with strong visible-light absorption and low reaction barriers. On the one hand, they demonstrated that B doping could reduce the band gap, thereby enhancing the light absorption and providing more excited electrons for PAS, while on the other hand, the dual active sites of Ti and B could synergistically promote the activation and reduction of N_2, as illustrated in Fig. 10b. G-C_3N_4, with good chemical stability under visible light, ease of preparation from simple raw materials, and environmental friendliness, has garnered widespread attention in the field of photocatalysis.[89] Li *et al.* doped Pt into Fe nanoclusters on various semiconductor surfaces, achieving a promising method for photocatalytic N_2 fixation to NH_3 under ambient conditions. The photocatalytic activity is highly sensitive to the electron density of the metal active sites and the surface band bending of the semiconductor. Studies have shown that adding small amounts of Pt^{2+} dopants can significantly alter the magnetic and electronic properties of Fe active sites, causing upward band bending on the semiconductor surface, which facilitates the transfer of photoelectrons from the semiconductor to adsorbed N_2. Therefore, the Mott–Schottky photocatalyst modified with FePt nanoclusters could enhance the electron-donating capability, providing an achievable pathway for efficient photocatalytic N_2 activation.[93]

The morphology of photocatalysts, including large surface areas, easily designed electron-transfer pathways, and exposed active sites, can influence the mass transfer, carrier transport, and reaction barriers in photocatalytic ammonia synthesis (PAS). Nanowires, with their high aspect ratios, nanoscale thickness and width, and microscale length, facilitate axial carrier transport, suppressing carrier recombination. Additionally, their large surface areas expose more active sites. Li and colleagues deposited Ru nanoclusters on the surface of n-type GaN nanowire arrays and found that the synthesized composite material exhibited significant photocatalytic activity for ammonia synthesis under UV irradiation at room

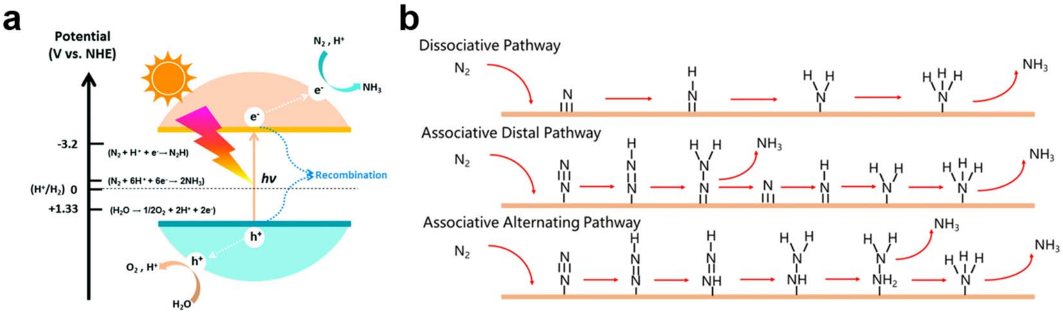

Fig. 9 (a) Schematic of the photocatalytic ammonia-synthesis reaction.[85] Copyright 2017, reproduced with permission from the Royal Society of Chemistry. (b) Schematic of the reaction mechanism of the ammonia-synthesis reaction.[86] Copyright 2023, reproduced with permission from the Royal Society of Chemistry.

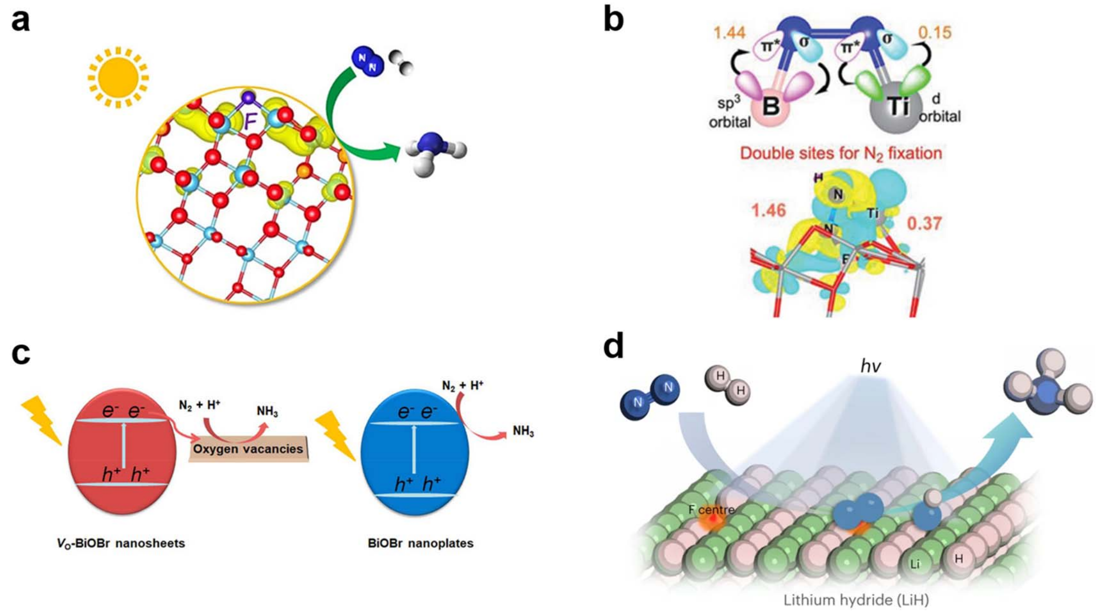

Fig. 10 (a) Schematic of the proposed mechanism for fluorine-induced surface metallization.[88] Copyright 2021, reproduced with permission from Wiley-VCH. (b) Simplified schematic of N_2 bonding to dual active sites of Ti and B.[89] Copyright 2023, reproduced with permission from Wiley-VCH. (c) Schematic of the photocatalytic ammonia-synthesis process on V_O-BiOBr nanosheets and BiOBr nanoplates.[90] Copyright 2018, reproduced with permission from American Chemical Society. (d) Schematic of the photocatalytic ammonia-synthesis process on LiH.[91] Copyright 2024, reproduced with permission from Springer Nature.

temperature. Because the work function of the n-type doped GaN is lower than that of Ru metal, electrons flow from the semiconductor into Ru, enhancing the electron-donating capability of Ru active sites and promoting the Ru-mediated cleavage of N≡N bonds, enabling low-temperature ammonia synthesis.[94]

Vacancies, a defect structure left when periodically arranged atoms or molecules are removed from the crystal, can significantly impact the performance of PAS. Constructing vacancies is a simple, efficient, and practical method to adjust the surface microenvironment, electronic structure, and chemical properties of photocatalysts. Vacancies can form defect energy levels, extending light absorption into the visible spectrum, capturing electrons, and facilitating carrier separation. Additionally, they can generate electron-rich or electron-deficient centers that serve as active sites for N_2 adsorption and activation. Xue *et al.* introduced oxygen vacancies (O_V) into BiOBr nanosheets by adding the polymer surfactant polyvinylpyrrolidone (PVP) (Fig. 10c). During the nucleation process, the added PVP binds to uncoordinated Bi atoms, reducing the surface energy and forming abundant O_V. After the introduction of O_V, the sample exhibited a redshift to 440–470 nm, showing enhanced absorption in the visible-light range, which benefits PAS applications.[90] Zhao *et al.* reported a Ru-loaded defective pyrochlore $K_2Ta_2O_{6-x}$ photocatalyst with significant visible-light absorption and an extremely low work function (similar to that of metallic magnesium). This photocatalyst could effectively drive the photocatalytic synthesis of ammonia from N_2 and H_2 under pressures as low as 0.2 atm. The photocatalytic rate was 2.8 times higher than that of the previously reported best photocatalysts, and the photothermal rate at 425 K was similar to that of Ru-loaded black TiO_2 at 633 K. Due to the higher photoinduced charge-separation efficiency and the higher conduction-band position, the reaction activity of the pyrochlore structure was 3.7 times that of the perovskite structure with the same chemical composition. The Schottky barrier at the $K_2Ta_2O_{6-x}$/Ru interface and spontaneous electron transfer further improved the photoinduced charge separation and accumulated energetic electrons to facilitate N_2 activation.[91] Guan *et al.* found that LiH, as an inorganic wide-bandgap semiconductor, undergoes dehydrogenation and a color change under UV irradiation. Unlike conventional oxide or nitride semiconductors, LiH loses electrons from hydride ions (H^-) to form H_2 after carrier separation, creating hydrogen vacancies. The photogenerated electrons can form electron-rich structures at surface hydrogen vacancies, aiding nitrogen reduction and activation. Negative hydrogen also participates in N–H bond formation in this process. Under N_2–H_2 co-feeding conditions, the team achieved photocatalytic ammonia synthesis using LiH under mild conditions (Fig. 10d).[95]

In most experimental studies on photocatalytic ammonia synthesis, the rate and yield of ammonia production remained low, indicating a significant gap from the demands of industrial application. Future research should focus on developing new catalysts, especially those with a higher light-absorption efficiency, longer photogenerated carrier lifetimes, and better reaction selectivity. In addition, synthesizing catalysts with multifunctional composite structures is another important direction. In summary, while photocatalytic ammonia synthesis is an emerging green technology with many advantages, it still faces challenges, such as insufficient activity, poor stability, and low efficiency. Future research should focus on addressing these issues to promote the practical application and commercialization of this technology.

3.2.5 Electrochemical ammonia synthesis. Electrochemical ammonia synthesis is an emerging and promising green technology.[96] In an electrochemical cell, the reduction of nitrogen (N_2) to ammonia occurs on the electrode surface. In simple terms, N_2 molecules are adsorbed onto the electrode surface, where they are reduced by electrons provided by an external circuit, and protons are added to form ammonia. The electrochemical ammonia synthesis (ECAS) methods can be categorized into five types based on the type of charge carriers used in the electrochemical cell, namely H-ECAS, N-ECAS, OH-ECAS, O-ECAS, and Li-ECAS. The characteristics of the charge carriers influence the operating temperature, electrolyte type, and corresponding electrode reactions. Compared to the Haber–Bosch process, the advantages of the electrocatalytic nitrogen-reduction reaction (NRR) for ammonia synthesis are as follows: (1) use of H_2O instead of H_2 as the hydrogen source, which reduces fossil fuel consumption, and the raw materials are non-toxic, harmless, and widely available;[13] (2) electrocatalytic NRR can break thermodynamic limitations by adjusting the operating potential; (3) the reaction conditions are mild, resulting in lower energy consumption and higher safety during the process; (4) the use of electrical power allows for the selection of renewable green energy sources, such as solar, wind, and geothermal energy; (5) the process is simple and flexible, requiring no expensive infrastructure, enabling ammonia synthesis facilities to be built in remote areas for on-demand and precise ammonia production, with significantly greater flexibility and tunability than the Haber–Bosch process.[97]

The main challenge for electrochemical ammonia synthesis is the low activity and selectivity of the currently available N_2-reduction electrocatalysts. In most electrochemical systems, the hydrogen-evolution reaction predominates, with most electrons and protons directed toward this reaction rather than the reduction of N_2 to ammonia, leading to a low faradaic efficiency. Although a high faradaic efficiency can be achieved at very low current densities, the ammonia-production rate remains low. Increasing the current density typically leads to a decrease in faradaic efficiency, as the electrocatalyst surface is primarily involved in hydrogen evolution, leaving few active sites for N_2 reduction.[98] Singh *et al.* analyzed the electrochemical N_2-reduction process using a qualitative model and noted that the ammonia-production rate is zero-order with respect to both the electron and proton concentrations, while the hydrogen-evolution rate is first-order with respect to both.[99] This suggests that limiting the availability of protons or electrons at the electrode surface could enhance the selectivity for ammonia. Consequently, the authors proposed four strategies to improve the selectivity of electrochemical ammonia synthesis. A potential method to avoid the hydrogen-evolution reaction is to decouple the reduction of N_2 from the subsequent protonation to form ammonia. In this context, lithium is the most widely studied medium, as metallic lithium reacts with N_2 at room temperature to form lithium nitride, which can further react with proton sources (such as water and ethanol) to generate ammonia. Therefore, lithium could theoretically serve as a medium for the electrochemical reduction of N_2 to ammonia. However, this process cannot be applied in aqueous solutions, as the onset potential for hydrogen evolution is significantly more positive than that for the reduction of Li^+ to Li, and lithium metal readily reacts with water to release H_2 gas. Thus, this reaction is typically conducted in non-protic solvents. One of the earliest examples of lithium-mediated N_2 reduction was presented by Tsuneto *et al.*, where ethanol was likely used as the proton source, while water was deemed an unfavorable proton source; and lithium played a crucial role in the N_2-reduction process.[100] Kim *et al.* employed a Li^+-conducting glass-ceramic membrane (LISICON) to separate a chamber containing a Ni cathode and organic electrolyte from a Pt/C anode and aqueous electrolyte.[101] Notably, no increase in the water content of the organic electrolyte was observed during the electrolysis, indicating that the LISICON membrane could prevent the mixing of the two electrolytes while allowing the transport of Li^+. However, the polarization curve of the electrochemical cell exhibited a linear behavior, necessitating a voltage greater than 5 V to achieve a reasonable current density, attributed to the low conductivity of the LISICON membrane. In the study by Lazouski *et al.*, as shown in Fig. 11b, lithium bis(trifluoromethanesulfonyl)imide was used as the electrolyte for Li-NRR, achieving a stable ammonia-production rate of 150 ± 20 mmol s^{-1} cm^{-2} and a nearly 100% faradaic efficiency.[102] A four-day continuous stability test was performed, which demonstrated the high operational stability of the system. The combination of a non-aqueous electrolyte system significantly enhanced the selectivity and electrochemical stability, enabling the electrochemical cell to operate over a wide range of potentials. Li *et al.* demonstrated a chain ether-based electrolyte capable of achieving long-term continuous ammonia synthesis, as illustrated in Fig. 11c.[104] The authors found that chain ether-based solvents possess non-polymerizable properties and a high boiling point (162 °C), and they could form a dense solid–electrolyte interface (SEI) on the gas-diffusion electrode (GDE), facilitating ammonia release in the gas phase and ensuring electrolyte stability. The authors demonstrated that under 1 bar and room temperature conditions, a 25 cm^2 electrode could be operated continuously for 300 h in a flow electrolyzer, achieving a current ammonia efficiency of $64\% \pm 1\%$ and a gas-phase ammonia concentration of approximately 98%, which was an unprecedented level. This work highlights the critical role of solvents in long-term continuous ammonia synthesis. Fu *et al.* confirmed the feasibility of Ca-mediated N_2 reduction for electrochemical ammonia synthesis (Ca-NRR), as shown in Fig. 11d.[105] The authors found that by using $Ca(BH_4)_2$ as the electrolyte at room temperature, metallic Ca could be electro-deposited onto the GDE. The metallic Ca then reacted with N_2, forming $Ca_xN_yH_z$ deposits on the electrode, which, when immersed in water, released ammonia. The indirect faradaic efficiency of $Ca(BH_4)_2$ was $28\% \pm 3\%$. Since $Ca(BH_4)_2$ reacts with the proton shuttle agent EtOH during Ca-NRR, making it incompatible with EtOH, the authors synthesized another calcium salt, $Ca[B(hfip)_4]_2$, by

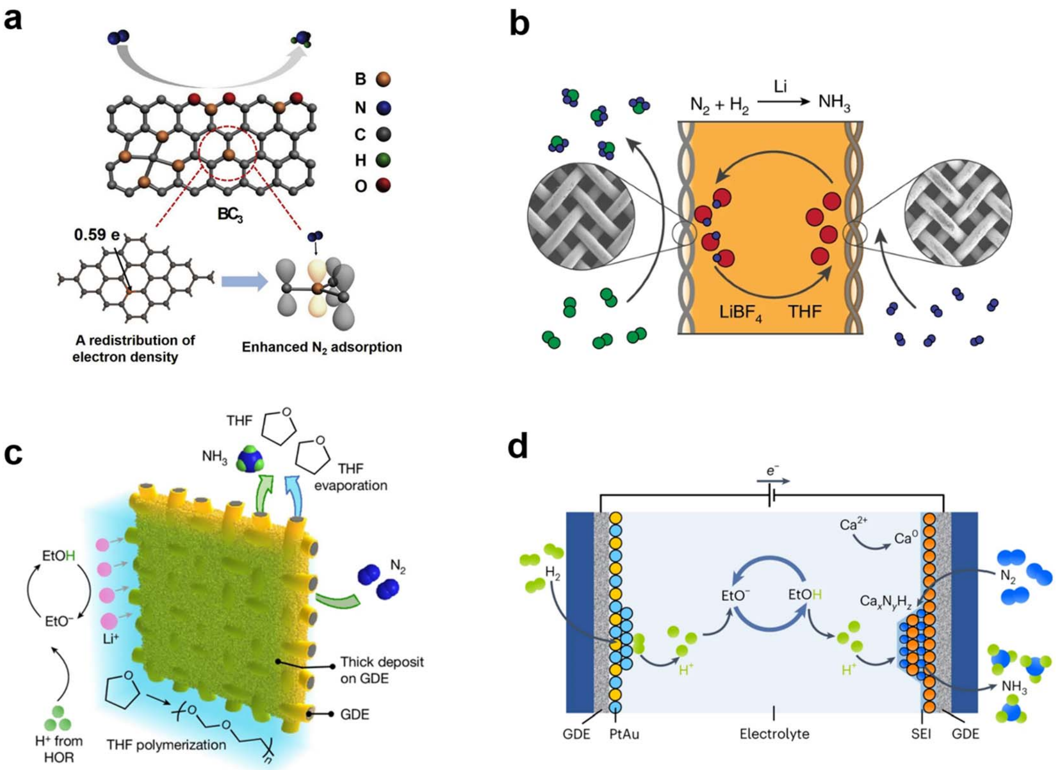

Fig. 11 (a) Schematic of the ammonia-synthesis process on BC_3.[103] Copyright 2018, reproduced with permission from Cell Press. (b) Method to overcome the transport limitations in tetrahydrofuran using a stainless-steel cloth-based support for ammonia synthesis paired with hydrogen oxidation.[102] Copyright 2020, reproduced with permission from Springer Nature. (c) Schematic of long-term electrochemical ammonia synthesis.[104] Copyright 2024, reproduced with permission from Springer Nature. (d) Schematic of the Ca-NRR in a flow cell.[105] Copyright 2024, reproduced with permission from Springer Nature.

reacting $Ca(BH_4)_2$ with hexafluoroisopropanol. $Ca[B(hfip)_4]_2$ was dissolved in THF as the electrolyte, with EtOH used as the proton shuttle, successfully achieving continuous Ca-NRR electrochemical ammonia synthesis in a flow cell. Under ambient conditions, the ammonia faradaic efficiency was 40% ± 2%. Quantitative $^{15}N_2$ isotope-labeling experiments and Ar blank tests confirmed that the ammonia produced during the Ca-NRR originated from N_2 reduction. This work is expected to inspire further exploration of other metals, such as Mg, Ba, Sr, and Na, for mediating N_2 reduction to ammonia. Such explorations will expand the range of options for efficient, selective, stable, economical, and scalable electrochemical fertilizer synthesis technologies.

Advanced catalyst design strategies include introducing vacancies, heteroatom doping, surface engineering, and alloying. These strategies can adjust the physical and chemical properties of catalysts at the atomic level, enhancing the affinity between nitrogen and adsorbed atoms while suppressing the hydrogen-evolution reaction (HER).[106,107] Heteroatom doping is one of the most practical methods to enhance the efficiency of NRR catalysts. Based on the type of heteroatoms, doping can be classified into metal doping and non-metal doping. The introduction of heteroatoms can effectively reduce the reaction barriers for the NRR and increase the number of active sites. Furthermore, many studies have shown that heteroatom doping can create more vacancies and modulate the active charge transfer, significantly improving catalyst efficiency. Zheng *et al.* used boron-doped graphene as an efficient non-metallic electrocatalyst for N_2 reduction. Boron doping in the graphene framework caused a redistribution of its electron density, with electron-deficient boron sites enhancing the binding ability to N_2 molecules, as shown in Fig. 11a.[103] Density functional theory (DFT) calculations revealed the catalytic activity of various boron-doped carbon structures, with the BC_3 structure showing the lowest energy barrier for the conversion of N_2 to NH_3. At a doping level of 6.2%, boron-doped graphene achieved an NH_3 production rate of 9.8 $\mu g\ h^{-1}\ cm^{-2}$, with a maximum faradaic efficiency of 10.8% at 0.5 V *vs.* SHE. This work demonstrated the potential of the designed electrocatalysts for efficient N_2 reduction.

4 Ammonia storage and transportation technologies

As an important industrial chemical and potential energy carrier, effective storage and transportation technologies for ammonia are critical to its economic viability and environmental impact. This section provides a detailed overview of liquid and solid-state ammonia storage, the transportation technologies, and the novel storage and transportation materials and methods, offering a comprehensive technical review.

4.1 Liquid-ammonia storage

Ammonia gas, with a relatively high density, is commonly stored and transported in liquid form. Compared to gaseous storage, liquid-ammonia storage has a higher volumetric density and greater transportation efficiency, making it one of the most commonly used methods for ammonia storage. Table 2 shows that ammonia's energy and power density are comparable to other non-fossil fuels. However, its most appealing advantage is its carbon-free nature.

Liquid ammonia must be cooled to below −33 °C to maintain its liquid state at room temperature.[111] This process typically involves refrigeration systems, and the storage tanks require good insulation to maintain a low-temperature environment.[112] Liquid storage significantly increases the storage density, thereby reducing space requirements. Liquid-ammonia-storage equipment includes pressure vessels and insulated tanks, typically made from high-strength steel or stainless steel, with lining materials for corrosion protection. For example, ammonia-storage tanks are coated internally with fluoride to enhance corrosion resistance. To prevent ammonia vaporization, storage tanks are usually equipped with pressure-regulation systems to maintain a constant internal pressure. Liquid-ammonia storage involves high safety considerations. Ammonia gas is toxic and irritating to humans, so storage facilities must be equipped with efficient ventilation systems and emergency response devices.[113] Storage areas should be located away from residential areas and undergo regular safety inspections and maintenance to ensure equipment operates properly.

4.1.1 Solid-state ammonia storage. To improve safety during storage and transportation, solid-state forms of ammonia storage have been developed.[114] Solid-state ammonia storage primarily involves the combination of ammonia with solid materials, such as metal salts or porous materials like polymer resins, silica gel, alumina, zeolites, carbon materials, as well as highly tunable porous materials like metal–organic frameworks (MOFs), covalent organic frameworks (COFs), hydrogen-bonded organic frameworks (HOFs), and porous organic polymers (POPs).[115–120] Absorbing ammonia into solid materials during transportation reduces the risks associated with traditional ammonia storage and transport.

From an economic perspective, advancements in solid-state storage technology have significantly increased ammonia storage density, reducing overall storage and transportation costs. Convenience is another major advantage of solid-state storage. Solid-state systems are usually simple to operate, and compared to gas-storage systems, the ammonia loading and unloading process is much safer. The stability of solid ammonia materials offers greater advantages during transportation. Solid-state storage effectively reduces ammonia volatilization and loss, making it suitable for international trade and long-distance transport. With further research, solid-state ammonia storage will play an increasingly important role in ammonia production and applications, driving the energy transition and further sustainable development. Future challenges lie in developing more suitable solid-state storage methods to adapt to a wider range of scenarios, with an aim to improve the sustainability of the absorption and release processes, maintain the stable cycling of solid materials, and explore new materials with enhanced ammonia-storage capacity.

4.1.2 Ammonia-transportation technologies. Ammonia-transportation technologies are crucial in its synthesis and utilization processes, and mainly involve gaseous and liquid transportation methods. Gaseous ammonia is typically transported over short distances through high-pressure pipelines, a relatively economical method but requiring high sealing and pressure resistance of the equipment to ensure safety and stability during transport. In contrast, liquid ammonia transport is more common and suitable for long-distance transport, typically using specialized liquid ammonia tankers and ships. Liquid ammonia is stored under low temperature and high pressure, effectively enhancing the transport efficiency and energy density, which is a major advantage. Nowadays, ammonia storage and transportation technologies have entered a highly developed stage. Ammonia has mature trade and transport infrastructure worldwide, along with highly developed high-density-ammonia-handling ports. Currently, the U.S. has over 10 000 ammonia-storage sites, connected by a pipeline network spanning more than 3000 km, linking the Gulf of Mexico to the Midwest. The Togliatti-Odessa pipeline, spanning 2471 km, is currently the world's longest ammonia pipeline.[121] Economically, while liquid-ammonia-transportation costs are relatively high, they are expected to decrease through large-scale transport and the introduction of new technologies. As transportation technology continues to advance, innovative transport methods, such as the use of autonomous vehicles and intelligent monitoring systems, will enable the real-time

Table 2 Power and energy densities of different hydrogen carriers in liquid form

Fuel	Boiling point (°C)	Weight% H_2 (%)	Power density (kW h kg^{-1})	Energy density (kW h L^{-1})	Ref.
Hydrogen	−253	100	33.3	2.54	8
Methanol	64.7	12.5	5.6	4.67	8
Ethanol	78.4	13	7.6	6.30	8 and 108
Ammonia	−33	17.6	5.2	4.32	8
Diesel	—	—	12.4	9.3	109
LPG (propane)	−42	18	14.8	8.3	110
LNG (methane)	−160	25	12.5–14.0	5.6–6.3	110

monitoring of transport conditions, further improving ammonia transport safety and efficiency. The use of new materials is also continuously reducing the weight and cost of transport equipment, making ammonia transportation increasingly viable.

5 Applications of ammonia

5.1 Direct applications of ammonia as a fuel

Ammonia is not only an essential raw material in modern industry, used in fuels, fertilizers, explosives, synthetic resins, pharmaceuticals, and other agricultural and industrial products, but also "green ammonia," synthesized without carbon emissions, is widely studied as a clean energy source due to its potential for hydrogen storage and combustion. In 2021, China announced ambitious goals to peak carbon dioxide emissions by 2030 and achieve carbon neutrality by 2060. Therefore, research into the direct use of ammonia as a fuel represents a significant development direction to aid meeting these goals.

5.1.1 Basic principles of ammonia-combustion technology. Hydrogen is the most abundant element in the universe, and hydrogen energy, as a high-energy, clean fuel, produces only water during combustion without generating other pollutants.[122] Thus, hydrogen energy, with its vast potential and appeal, is regarded as a highly promising future energy source. Gaseous H_2 has a relatively high energy density (142 MJ kg^{-1}), while the volumetric energy content of liquefied hydrogen is 8.5 MJ L^{-1}.[123] Despite this, the widespread use of hydrogen energy still faces many unresolved challenges, such as storage, transportation, liquefaction, and safety concerns, including its flammability and explosiveness.[124]

To meet the growing energy demands, it is imperative to find a "green energy" alternative to hydrogen. Ammonia, as a carbon-free fuel, offers various advantages, such as mature production technology, ease of storage and transportation, and zero CO_2 emissions during combustion, making it a strong contender to replace fossil fuels.[125] With an energy density of approximately 22.5 MJ kg^{-1}, ammonia compares well to fossil fuels like coal (20 MJ kg^{-1}), natural gas (55 MJ kg^{-1}), liquefied natural gas (54 MJ kg^{-1}), hydrogen (142 MJ kg^{-1}), ethanol (27 MJ kg^{-1}), gasoline (44 MJ kg^{-1}), and diesel (37 MJ kg^{-1}), making it highly suitable for direct use as a fuel.[126]

Since the 1950s, many fundamental studies have been conducted to understand the combustion characteristics of ammonia. However, ammonia is considered to have certain limitations in its combustion properties due to its low flame speed, high ignition energy, narrow flammability limits, and low flame temperature. To address these issues, blended combustion methods are commonly used in combustion equipment.

For mixed fuels, the ignition delay time (IDT) is a key parameter in combustion research. It describes the time taken for a fuel–oxidizer mixture to reach a sustained combustion state (ignition).[127] This metric is crucial for understanding and designing the combustion process, as it directly impacts the combustion response time, efficiency, and product distribution. It is influenced by several variables, including the initial temperature, pressure, fuel–oxidizer ratio, and specific components in the gas mixture. By precisely controlling the ignition delay time, the performance of combustion systems can be significantly improved while reducing harmful emissions. The laminar burning velocity (LBV), also known as the laminar flame speed, is another key parameter, like IDT, in the study of fundamental gas-combustion principles. LBV measures the rate at which the flame front propagates through a fuel–oxidizer mixture under stable flow conditions. It is defined as the rate of flame propagation along the mixture in the absence of turbulence, measured in meters per second (m s^{-1}). This parameter reflects the combustion efficiency of the fuel–oxidizer mixture in a calm environment and is a critical indicator for assessing combustion stability and the flame-propagation characteristics.[128] Measurements of the laminar flame-propagation rates for ammonia mixtures began in the early 1950s, using Bunsen flame methods in laboratory combustion devices.[129] At the same time, the flammability limits of mixed fuels are also critical physical properties in the study of ammonia combustion. The flammability limits refer to the concentration range within which a combustible gas or vapor can sustain combustion when mixed with air under specific conditions. As the initial temperature increases, the combustion temperature of ammonia decreases at the lower flammability limit (LFL) and increases at the upper flammability limit (UFL). As the initial pressure increases, the flame temperature decreases at the LFL and increases at the UFL. In summary, ammonia's flammability limits are influenced by various factors, including the type of diluent, ambient temperature, operating pressure, and ammonia concentration. Understanding how these variables affect the ammonia-combustion behavior is essential for developing safety measures, predicting combustion boundaries, selecting appropriate fire-suppression strategies, and assessing potential risks associated with ammonia leakage.

Fundamental studies on ammonia-combustion science are of great significance, providing valuable data to support the future development of ammonia as a clean energy source. With further research into ammonia' combustion characteristics, we anticipate breakthroughs in enhancing energy efficiency, reducing emissions, and advancing sustainable energy solutions.

5.1.2 Ammonia-combustion mechanism and kinetics research. As ammonia gains more attention as a potential sustainable energy source and a fuel alternative in the transportation sector, researchers have focused on the oxidation reactions of ammonia under mid-to-low temperatures (800–1600 K) and high pressures (over 2 MPa). These conditions match the operating environments of modern combustion devices, such as internal combustion engines. To develop ammonia-based combustion technologies, it is essential to understand the detailed chemical processes through combustion phenomena. Therefore, research on the kinetics of ammonia combustion is crucial.[130] Ammonia not only acts as a key intermediate in the devolatilization of solid fuels and the conversion of cyanides at high temperatures, but it is also used as a reducing agent in selective non-catalytic reduction (SNCR) to reduce nitrogen oxide (NO) emissions, a process known as thermal de-NO_x.[131]

Over the past few decades, various chemical kinetic models have been developed to simulate ammonia combustion under different conditions. However, limited by the available experimental data and specific application goals, none of the models can comprehensively and accurately predict all relevant scenarios. Lindstedt *et al.*,[132] Miller *et al.*,[133] and Bian *et al.*[134] have established fundamental theoretical frameworks for ammonia combustion and oxidation processes.

Miller *et al.* conducted an in-depth study on the chemical kinetics of ammonia combustion, arriving at several key conclusions essential for understanding the combustion characteristics of ammonia as a fuel. Their theoretical model shows good agreement with experimental observations in most cases, particularly under lean combustion conditions (equivalence ratio less than 1), but additional pyrolysis steps may be needed under fuel-rich conditions (equivalence ratio greater than 1.3). In the combustion of ammonia, nitric oxide (NO) formation primarily occurs through the nitroxyl (HNO) intermediate. In lean flames, NO is generated from the reactions between ammonia (NH_3) and oxygen atoms, or between nitrogen-hydrogen intermediates (NH) and hydroxyl and oxygen molecules. The conversion of NO to nitrogen (N_2) mainly proceeds through intermediates such as N_2O. Under fuel-rich conditions, ammonia and nitrogen-hydrogen intermediates rapidly convert to nitrogen atoms, which then form high-temperature NO and N_2 *via* the extended Zeldovich mechanism. While the theoretical model can effectively predict the flame structures, further research is needed to improve the accuracy of NO and N_2 predictions under fuel-rich conditions.[133]

Lindstedt *et al.* provided a detailed reaction mechanism that could accurately predict ammonia's oxidation behavior under various combustion conditions. Their study analyzed ammonia's oxidation pathways in flames, including the formation and consumption of key intermediates, like NH_2, NH, and NO. Their study particularly emphasized the relative importance of NO formation pathways under different flame conditions and the main routes for converting NO to N_2. It was found that the reaction between NH_2 and O is the primary source of NO formation, while NO reduction mainly occurs through its reaction with NH_2. This mechanism not only aids in optimizing SNCR technologies to reduce NO_x emissions but also serves as a guideline for designing more efficient and environmentally friendly combustion systems.[132]

Bian *et al.* developed a simplified kinetic mechanism using minimal estimated rate constants. Their model could successfully predict the molar fractions of nitrates and nitrites in experimental studies. In ammonia-doped flames, the production of NO and N_2O is primarily driven by the imino radical (NH), with the conversion rate of NH_2 to NH indirectly controlling the remaining NO and N_2O in the combustion gases. The temperature dependence of this reaction helps explain why ammonia is less effective at reducing NO at temperatures above 1400 K.[134]

Junichiro Otomo and colleagues proposed an improved model (UT-LCS model) that could accurately explain the reported values of laminar flame speeds and ignition delay times over a wide range of equivalence ratios and pressures. Additionally, this model was applied to demonstrate NH_3/H_2/air combustion, successfully predicting the laminar flame speeds of NH_3/H_2/air as a function of the equivalence ratio.[135] This model could satisfactorily explain both the flame speeds and ignition delay times in ammonia combustion. The improvements included considerations of the reactivities of NH_2, HNO, and N_2H_2, which play key roles in refining the ammonia-oxidation mechanism. Moreover, the model successfully predicted the flame speeds in NH_3/H_2/air combustion, providing strategies for more efficient ammonia combustion in the future.

In the traditional Zeldovich mechanism, NO_x is primarily formed through the oxidation of NH radicals. However, due to the unique chemical properties of ammonia, the NO_x-formation process in ammonia combustion is more complex, involving ammonia decomposition, oxidation, and reactions with other intermediates. Under fuel-rich conditions, downstream NO concentrations are significantly reduced, and large amounts of H_2 are generated, which can thermally reduce NO_x, creating a low-NO_x/NH_3 emission window. In these reactions, a relatively high concentration of NH_2 is observed, playing a key role in NO reduction.[135] Under lean conditions, downstream NO concentrations are high. H_2 is produced at the flame front but burns in the post-flame zone. Researchers predict that the extended Zeldovich mechanism could reduce NO emissions in fuel-rich NH_3/air flames.[136] Additionally, researchers have proposed various strategies, such as active fuel doping and pre-cracking, to enhance the ammonia-combustion reactivity while reducing pollutant emissions. However, the low-emission window for ammonia combustion is very narrow, and enhancing strategies on the fuel side can often lead to trade-offs in pollutant emissions. This makes the simultaneous regulation of the ammonia-combustion activity and pollutant emissions a major challenge in the field of ammonia energy.

5.1.3 Ammonia fuel cells. Traditional energy technologies, which primarily rely on the combustion of fossil fuels, are no longer sufficient to meet the world's growing energy demands. This situation has driven an urgent search for various sustainable energy alternatives. Renewable sources, such as solar and wind energy, have been proposed and have shown the potential to replace traditional energy sources. Faced with the dual challenge of reducing greenhouse gas emissions and diversifying energy supplies, fuel cell technology has attracted widespread attention due to its clean, efficient electricity production, and as it is suitable for both static and dynamic applications. This is primarily due to its higher energy-conversion efficiency and lower environmental pollution. The development of fuel cell technology offers the possibility of creating novel thermodynamic systems that could generate electricity electrochemically using externally supplied reactants. Fuel cells efficiently convert the chemical energy of fuels and oxidants directly into electrical energy without being limited by the Carnot cycle, with efficiencies exceeding 90%.[137] At the same time, fuel cells are favored for their exceptional efficiency, smaller environmental footprint, and advanced characteristics that allow the direct conversion of fuel into electricity.

Fuel cells are categorized as follows: Proton Exchange Membrane Fuel Cells (PEMFCs), which include Direct Formic Acid Fuel Cells (DFAFCs) and Direct Ethanol Fuel Cells (DEFCs); Alkaline Fuel Cells (AFCs), which include Proton Ceramic Fuel Cells (PCFCs) and Direct Borohydride Fuel Cells (DBFCs); Phosphoric Acid Fuel Cells (PAFCs); Molten Carbonate Fuel Cells (MCFCs); Solid Oxide Fuel Cells (SOFCs); and Direct Methanol Fuel Cells (DMFCs).[138] Among these, proton ceramic fuel cells, solid oxide fuel cells, and alkaline fuel cells can be used for power generation with ammonia as the feedstock.[139] Given that direct ammonia fuel cell (DAFC) technology is still immature, it will not be discussed in detail in this section.

In fuel cell systems, hydrogen is the most commonly used fuel, though it has a low volumetric density of about 0.0813 g L^{-1} (at 25 °C and 1 bar).[140] Due to the high temperature and pressure required for hydrogen storage and transportation, several alternative approaches have been developed, such as using carbon-based liquid-hydrogen carriers, like methanol, which is applied through steam reforming in High-Temperature Polymer Electrolyte Membrane Fuel Cells (HT-PEMFCs).[141] However, since carbon-based fuels produce carbon dioxide during combustion, they are not highly attractive as fuel cell feedstocks. Ammonia, as an alternative carbon-free fuel source, has garnered widespread attention because it produces no carbon dioxide emissions during use.[125] Ammonia is relatively safe to store, liquefying easily at ambient temperature and around 10 atmospheres or at atmospheric pressure and −33 °C. Compared to other fuels, ammonia is less flammable, and any leakage can be easily detected by its distinctive odor, enhancing its safety as a fuel.

Due to the unique operational mechanism of fuel cells, nitrogen in the fuel stream merely serves as a diluent for hydrogen, generating no pollutants nor causing significant performance degradation. This characteristic makes fuel cells compatible with ammonia and allows them to be operated safely and efficiently.[141] In the anode of the fuel cell, ammonia participates in a triphasic reaction, generating nitrogen, with the nitrogen cycle supported by an additional loop. Nitrogen, which is easily sourced from the air, plays a supporting role in the chemical synthesis process, where the Haber–Bosch process is commonly used for production. As energy is released, nitrogen is ultimately discharged harmlessly into the atmosphere, ensuring a zero-carbon emission system.[142]

Among the various types of fuel cells, Solid Oxide Fuel Cells (SOFCs) are particularly well-suited to using ammonia as a fuel.[143] SOFCs offer various advantages, such as high efficiency, fuel flexibility, low emissions, high-temperature operability (stably functioning at temperatures above 1000 K), solid-state structure, rapid startup, and load responsiveness, making them a highly efficient and promising energy-conversion technology.[144]

In an ammonia fuel cell system, ammonia is first decomposed into nitrogen and hydrogen at the anode, catalyzed by the electrocatalyst. The efficiency of this process depends on the catalyst performance and typically occurs at elevated temperatures. Fig. 12a and b provides detailed illustrations of typical setups for direct ammonia fuel cells and ammonia electrolysis cells.[145] In theory, ammonia undergoes decomposition at 500–1000 K, and SOFCs are often applied in scenarios exceeding 1000 K.[148] At high temperatures, the decomposition and power generation processes can occur simultaneously. Therefore, ammonia can be directly fed into SOFCs for energy conversion without requiring pre-treatment.[149] Ganley and colleagues reported on the feasibility of SOFCs, as illustrated in Fig. 12c.[146] Depending on the membrane type used in the cell, two different types of SOFCs can be distinguished: (1) proton exchange membranes (SOFC–H) or (2) anion exchange membranes (SOFC–O). For direct ammonia SOFC–O (where “O” denotes oxygen ions permeating through the membrane), oxygen is split into O^{2-}, which migrates to the anode and reacts with H_2 to form water. Conversely, for direct ammonia SOFC–H (where “H” denotes hydrogen ions permeating through the membrane), hydrogen produced at the anode is split into H^+ and electrons, which react with oxygen at the cathode to form water.[147]

The electrolyte in SOFCs is typically made of solid ceramics composed of metal oxides, with YSZ (yttria-stabilized zirconia) being a commonly used electrolyte.[148] YSZ was first applied in ammonia fuel cells by Vayenas and Farr. Solid electrolytes offer several advantages, such as eco-friendliness, ease of maintenance, high conductivity, the ability to operate at high temperatures, and low energy requirements, all of which help enhance electrolysis efficiency and reduce costs.[150] In 2006, G. G. M. Fournier and colleagues conducted detailed experimental studies on the characteristics of ammonia fuel cells to determine the optimal operating conditions and design parameters for implementing direct ammonia fuel cells. They tested three different electrode materials—silver, platinum, and nickel-ceramic composites—and two types of solid electrolyte materials, namely CaSZ and YSZ. Their performance across the full range of current densities was studied, demonstrating that direct ammonia fuel cells produced higher power density compared to hydrogen-driven fuel cells. The study revealed that ammonia could achieve higher power densities than hydrogen, with the difference being 11 mW cm^{-2} in favor of ammonia at 1073 K. This indicates that fuel cell systems supported by ceramic-metal composite anodes are ideal for directly using ammonia as fuel.[151]

At the anode of fuel cells, the use of highly selective catalysts is critical to ensure that the ammonia-oxidation reaction exclusively produces nitrogen, avoiding the generation of nitrogen oxides. In recent years, anode materials for ammonia fuel cells have been roughly categorized into two types: (1) noble metal materials, such as platinum-based materials, and (2) non-noble metal materials, such as nickel-based and iron-based materials.[152] More research has been focused on non-noble metal materials due to their ability to avoid the high costs associated with noble metals like platinum. Wojcik *et al.* suggested that iron-based catalysts could directly decompose NH_3 into N_2 and H_2, and if this reaction proceeds more rapidly than the reaction forming NO, the selectivity for NO could be reduced to zero.[149] Masashi Kishimoto and colleagues conducted experimental studies on the ammonia-decomposition rate on conventional porous Ni-YSZ anodes in SOFCs. Their study found that the decomposition rate depended not only on the

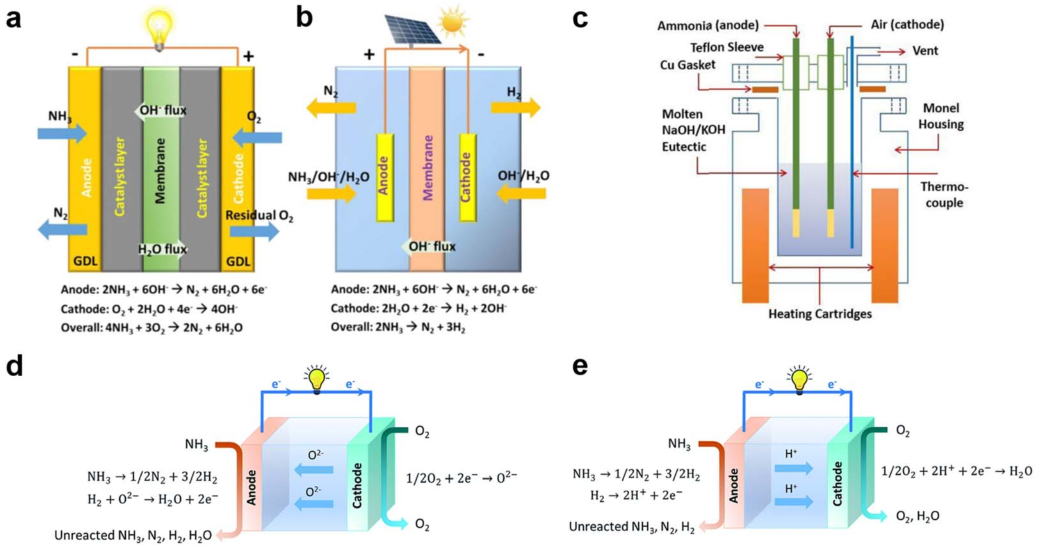

Fig. 12 (a) Schematic of a typical direct ammonia fuel cell, where water is produced as a byproduct. (b) Schematic of a typical ammonia electrolysis cell for hydrogen generation.[145] Copyright 2018, reproduced with permission from IPO Science. (c) Schematic of a direct ammonia fuel cell using molten hydroxide as the electrolyte.[146] Copyright 2007, reproduced with permission from Elsevier. (d) and (e) Schematic of an ammonia-fed SOFC–O and ammonia-fed SOFC–H.[147] Copyright 2013, reproduced with permission from the Royal Society of Chemistry.

partial pressure of ammonia but also on the partial pressure of hydrogen under typical SOFC operating conditions, with higher hydrogen concentrations significantly reducing the decomposition rate.[153] Despite the good catalytic activity shown by nickel-based catalysts, they may face corrosion issues during long-term operation, potentially reducing the overall efficiency of the fuel cell. Catalyst activity, selectivity, stability, and cost are the main factors limiting the commercial application of fuel cells. As a result, researchers are exploring ways to optimize the structure of nickel-based catalysts through alloying or other surface-sensitive synthesis methods to enhance their stability and performance.

5.2 Ammonia cracking for hydrogen production

During the transition from fossil fuels to renewable energy, hydrogen is considered an effective low-carbon alternative. However, due to the chemical and physical properties of hydrogen, the costs associated with its storage and transportation are relatively high. As a result, researchers are exploring other compounds to act as hydrogen carriers, with an aim to improve the economic efficiency. Ammonia has emerged as a strong contender in this field due to its high energy density, and ease of storage and transportation. Although large-scale ammonia cracking technology is not yet fully developed, many researchers are actively working on advancing this area.

At the active sites, the decomposition of ammonia begins with a stepwise dehydrogenation process after ammonia is adsorbed onto the active sites. While nitrogen adsorption is often regarded as the rate-determining step in ammonia synthesis, the rate-determining step for ammonia decomposition varies depending on the metal active site. For noble metals, such as Ru and Rh, the dissociation of the nitrogen–hydrogen bond (N–H bond) is the rate-determining step, whereas, for non-noble metals, like Fe, Co, and Ni, nitrogen desorption is the rate-determining step.[154] The catalyst plays a critical role in ammonia decomposition for hydrogen production, as it can significantly increase the reaction rate, reduce the reaction temperature and activation energy, and selectively promote hydrogen production.[155] Ganley and colleagues experimentally investigated the catalytic activity order of 13 different metals from the periodic table. The results showed the following catalytic activity order: Ru > Ni > Rh > Co > Ir > Fe ≫ Pt > Cr > Pd > Cu > Te, Se, Pb.[156] In current research, the ammonia-decomposition mechanism catalyzed by transition metal active sites is consistently influenced by the metal-nitrogen (M–N) bond. On the one hand, a stronger M–N bond facilitates dissociation of the N–H bond but hinders nitrogen desorption and recombination, while on the other hand, a weaker M–N bond promotes nitrogen desorption and recombination but impedes N–H bond dissociation. An optimal metal–nitrogen bond is needed, one that not only facilitates N–H bond dissociation but also allows for the desorption of adsorbed nitrogen atoms.[157]

Among various transition metal catalysts, ruthenium has garnered significant attention for its exceptional ammonia-decomposition capabilities, making it a focal point in ammonia-decomposition catalyst research. Given the high cost of precious metals, current research is focused on developing supported ruthenium nanoparticle catalysts to reduce ruthenium usage while achieving higher catalytic efficiency. The choice of support plays a crucial role in the design of supported ruthenium catalysts. Generally, different supports can alter the size, electronic structure, and crystalline form of ruthenium nanoparticles, providing an effective means of enhancing the activity of ruthenium-based catalysts.[155] Extensive experimental and theoretical computational results have shown that nitrogen dissociation and recombination are closely related to the unique B5 site, a stepped arrangement of five Ru atoms on the Ru (0001) surface. The B5 site typically forms a single atomic step arrangement on the Ru (0001) platform, consisting of three Ru atoms in one layer and two atoms in the layer directly above.[158] In 2004, Yin *et al.* studied the catalytic ammonia decomposition of Ru nanoparticles supported on CNTs for hydrogen production. Their results showed that due to the high graphitization of CNTs, which are inherently semiconducting and conductive, electron transfer from electron promoters to Ru was more effective on CNTs compared to with MgO and AC, showing enhanced nitrogen recombination and desorption.[159] Although carbon supports help improve Ru dispersion and provide good conductivity, they still face various issues, such as high cost, decomposition, and reactivity with ammonia.[160] In recent decades, metal oxides have been widely used as supports for ammonia-decomposition catalysts due to their abundant surface oxygen vacancies, surface acidity, and redox properties. Karim *et al.* first demonstrated that the number of Ru active sites (here, the B5 site) strongly depends on the particle shape and increases with the particle size. Due to polydispersity, the optimal particle size for hemispherical particles is 2–3 nm (as shown in Fig. 13a), which corresponds to the maximum concentration of B5 sites. The results clearly showed that ammonia decomposition on Ru was highly structure-sensitive, with TOF values increasing by nearly two orders of magnitude as the particle size increased from 0.8 nm to greater than 7 nm.[165] Despite extensive efforts to increase the number of B5 sites in ruthenium-based ammonia-decomposition catalysts, their high cost remains a significant limitation.[155] Additionally, traditional ruthenium-based supported catalysts tend to suffer from hydrogen poisoning under mild reaction conditions.[161] Therefore, the hydrogen-transfer ability at the support interface in contact with the B5 sites is crucial. Hayashi *et al.* used the inorganic electride C12A7:e$^-$ as a support, which significantly enhanced nitrogen recombination and desorption due to its high electron-donating capability and resistance to hydrogen poisoning. Moreover, the turnover frequency (TOF) of H_2 formation on this catalyst was approximately four times higher than that of K–Ru/AC. Among the essential properties of an ideal support, the electron-donor capability is considered the most critical.[166,167] Fang H. *et al.* investigated the ammonia-decomposition performance of Ru on various MgO crystal planes. Their results clearly demonstrated the superior performance of Ru/MgO(111) catalysts (as shown in Fig. 13b). Under specified ammonia-flow rates, metal loadings, and temperatures, the specific activity of Ru on different supports was compared. The results indicated that supports with hydrogen-transfer capabilities exhibited significantly higher ammonia-decomposition abilities compared to inert materials.[162] Similar to CNTs, zeolites are electron-rich materials. Kwan Chee Leung *et al.* exchanged Ru with Na ions in 13X zeolite, resulting in a catalyst that confined Ru within the 13X zeolite cavities. Compared to most catalysts reported in the literature, this catalyst exhibited the highest specific catalytic activity for NH_3 decomposition, exceeding 4000 h^{-1}, with a lower activation barrier. Inside the zeolite cavity (as shown in Fig. 13c), Ru formed a confined Lewis acid–base pair with the oxygen atoms in the zeolite cavity, which helped activate small molecules like ammonia, promoting N–H bond dissociation. Additionally, the electron-rich zeolite facilitated electron transfer for nitrogen desorption.[163]

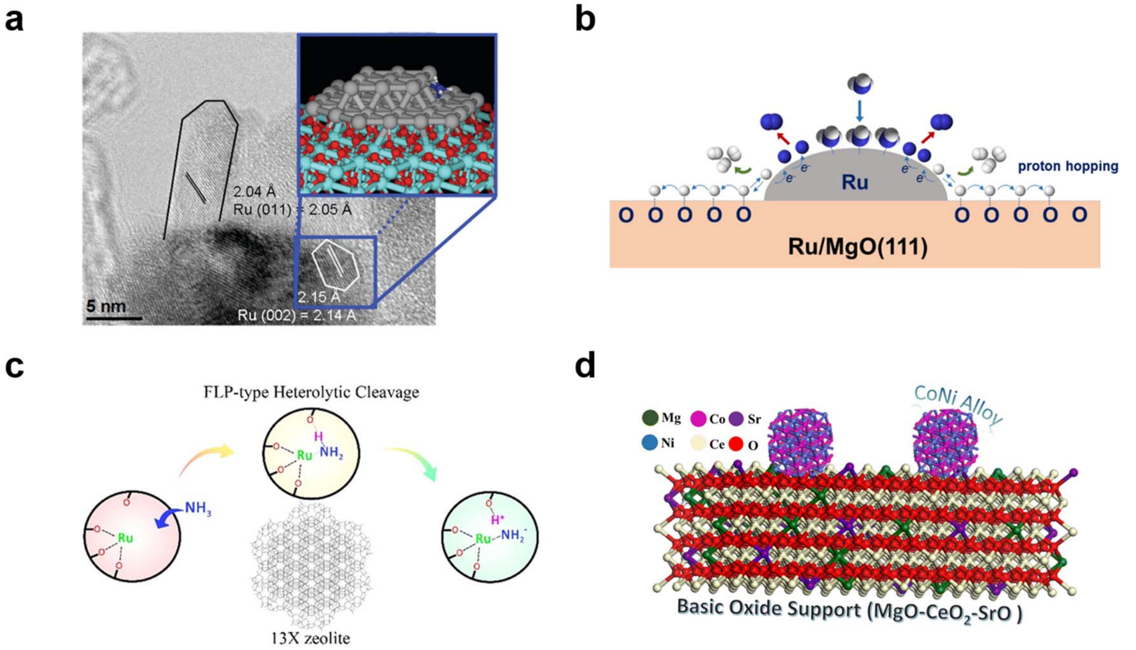

Fig. 13 (a) Schematic of the B5 site on the Ru/Al_2O_3 catalyst.[161] Copyright 2009, reproduced with permission from American Chemical Society. (b) Hydrogen-transfer behavior in Ru/MgO(111).[162] Copyright 2023, reproduced with permission from Springer Nature. (c) FLP-type mechanism of N–H cleavage between NH_3 and Ru sites in Ru-13X zeolite.[163] Copyright 2023, reproduced with permission from American Chemical Society. (d) Schematic of a Co–Ni alloy decorated on MgO–CeO_2–SrO.[164] Copyright 2022, reproduced with permission from Royal Society of Chemistry.

Among the various transition metals, although ruthenium-based catalysts exhibit the best performance for ammonia decomposition, their high cost hinders their commercial application and widespread adoption. Therefore, finding transition metals that can replace Ru as commercial catalysts is a key focus of ammonia-decomposition research. Tabassum *et al.* designed a Ru-free catalyst with a heterogeneous structure, consisting of cobalt–nickel alloy nanoparticles dispersed on a mixed oxide support of MgO–CeO_2–SrO (as shown in Fig. 13d). At 450 °C, the catalyst achieved ammonia conversion efficiencies of 97.7% and 87.5% at gas hourly space velocities (GHSV) of 6000 and 12 000 mL h^{-1} $g_{cat}{}^{-1}$, respectively. At 500 °C, the hydrogen-production rate was comparable to that of most reported ruthenium-based catalysts.[164]

To achieve stronger SMSI (strong metal–support interaction), various types of supports have been extensively developed and studied. The results showed that highly basic, electron-conductive supports can promote the performance of highly efficient ruthenium- or nickel-based catalysts, as basicity is critical for electron enrichment at active sites. Promoters are usually added as electron donors to facilitate nitrogen desorption during NH_3 decomposition. Catalyst preparation methods could be expected to alter the physical and chemical properties of the resulting catalysts, thereby affecting their catalytic performance.[160,168]

In the future, the application of ammonia-decomposition catalysts will not be limited to large-scale hydrogen production; their use is expected to extend to other areas too, such as automotive and marine power, remote area power supply, base station power, backup power, and distributed power stations.[169] These applications will contribute to the development of a "hydrogen energy society" and play a vital role in ensuring national energy security and achieving carbon neutrality. Additionally, as scientific research progresses and technological advancements continue, the performance of ammonia-decomposition catalysts will be further improved, and costs will be reduced, driving the rapid development of the hydrogen energy industry. Moreover, research on ammonia-decomposition catalysts will also promote technological advancements in related fields, such as hydrogen-storage materials, fuel cell technology, and chemical looping technology. The cross-fusion of these technologies will provide more opportunities for the application of ammonia-decomposition catalysts, further driving innovation and development in clean energy technologies. It is thus envisioned that ammonia-decomposition reactions will play a critical role in driving the global energy transition and achieving sustainable development goals.

6 Ammonia energy system challenges

6.1 Technical limitations and risks

In the pursuit of sustainable energy solutions, ammonia has garnered attention due to its unique chemical properties and energy potential. As a clean, efficient energy carrier, ammonia's role in energy transition is increasingly being recognized. However, the application of ammonia energy still faces various challenges, ranging from production, storage, transportation, to end-use, all of which pose technical, economic, and environmental concerns.

Compared to traditional fuels, such as gasoline or diesel, ammonia exhibits inferior ignition and combustion performance. Ammonia requires specific temperature and pressure conditions to ignite, and its slower combustion rate could lead to reduced engine efficiency and power output.[170] Moreover, ammonia's safety issues cannot be overlooked. It is corrosive and flammable under certain conditions, necessitating strict safety measures during its production, storage, transportation, and usage. Ammonia exists as a gas at atmospheric conditions but is typically transported in liquid form due to its higher density. Liquid ammonia can be transported through pipelines, tankers, and ships, usually cooled to approximately −33 °C, enabling transportation in non-pressurized containers.[111] These mild storage conditions are advantageous for both storage and transportation, allowing ammonia to benefit from the utilization of the existing liquid-energy-transport infrastructure, which is relatively well established.[171] However, ammonia's corrosiveness remains a critical concern. For non-metallic materials, like rubber or plastic, liquid ammonia can cause erosion, hence nitrile rubber is commonly used as a sealing material. In the presence of carbon oxides, gaseous ammonia poses severe corrosion risks, as only 5 ppmv of ammonia can lead to the formation of ammonium carbonate, further leading to hydrogen embrittlement at high pressures (15.0–20.0 MPa) and elevated temperatures (above 770 K).[139] Despite having a higher autoignition temperature (923 K) compared to hydrogen (793 K), methane (903 K), and propane (723 K), making it relatively safer, ammonia's toxicity is a significant issue. Its vapor pressure at room temperature is relatively high, making it about a thousand times more toxic than gasoline or methanol.[111] At ambient temperatures, liquid ammonia's hazards are significantly higher than other fuels, with an immediately dangerous to life or health concentration (IDLH) of approximately 300 ppm.[172] Additionally, ammonia usage at high temperatures can promote the formation of nitrogen oxides (NO_x), necessitating stringent control of the combustion process to mitigate pollution. As ammonia is classified as a toxic chemical, appropriate risk management measures are crucial to minimize potential harm to humans and the environment, which remain a major barrier to its widespread use.

6.2 Economic feasibility and sustainability assessment

As the global energy landscape shifts toward low-carbon alternatives and with the increasing focus on greenhouse gas reduction, ammonia, as a hydrogen carrier, has attracted considerable attention. Its high energy density, ease of storage, and potential for zero-carbon emissions make ammonia an attractive alternative fuel.[111] However, its economic feasibility is crucial to its widespread adoption.

Currently, about 80% of ammonia production is used for fertilizers, with 5% used for explosives and 15% for other chemicals.[173] Ammonia-production costs remain relatively low, particularly when coal is used as a feedstock in the Haber process, with costs ranging from \$147 to \$432 per ton, translating to a gasoline equivalent of \$0.96 to \$2.83 per gallon. Ammonia produced from natural gas or ocean thermal energy conversion (OTEC) is more expensive than coal-based production. Studies by Leighty and Holbrook evaluated the use of secondary energy sources, such as wind power for ammonia production, factoring in storage and transport costs. Their analysis estimated that delivered ammonia fuel costs would range between \$450 to \$650 per ton.[174] Furthermore, ammonia's transportation through pipelines is more efficient and cost-effective than hydrogen, with respective efficiencies of 93.4% for ammonia and 86.9% for hydrogen over a 1610 km distance. The storage cost advantages of ammonia are notable, requiring nearly five times less energy than hydrogen for cryogenic storage. When considering carbon-neutral pathways, ammonia offers lower energy costs from production to storage compared to hydrogen and methanol.[171]

Despite ammonia's lower flammability, its storage in liquid form poses risks. When storage temperatures increase, liquid ammonia vaporizes, raising pressure within the container and potentially leading to explosions.[175] While the complete combustion of pure ammonia theoretically yields N_2 and H_2O, this is nearly impossible to achieve in practice.[176] As discussed in the section on the ammonia-combustion kinetics, incomplete combustion tends to occur, producing significant NO_x emissions, especially under lean-fuel and high-temperature conditions.[135] These emissions pose environmental hazards, contributing to issues like acid rain, ozone depletion, photochemical smog, and air pollution.[170] Nonetheless, ammonia-combustion-related pollution problems can be mitigated. Sun *et al.*'s simulation study analyzed the effectiveness of selective catalytic reduction (SCR) technology in controlling NO_x and ammonia emissions from dual-fuel engines. They found that introducing additional air or oxygen into the SCR system could significantly reduce unreacted ammonia and NO_x emissions.[177] Similarly, Ziaur Rahman's research showed that pressurized oxygen combustion (POC) could control NO_x formation during ammonia combustion. They reported that as the pressure was increased from 1 atm to 15 atm, NO formation decreased from 43% to 76%, promoting the conversion of NO to N_2 at higher pressures.[178] It is anticipated that pollution issues associated with ammonia energy will be effectively resolved in the near future.

7 Prospects and outlook

7.1 Role of ammonia in future energy systems

Ammonia (NH_3), as an important chemical raw material, shows immense potential in future energy systems. Traditionally, ammonia is primarily used in the production of fertilizers and chemicals. However, with the rapid development of the global energy transition, ammonia can play a vital role in clean energy systems. Ammonia has a high energy density, favorable storage and transport characteristics, and its synthesis process can be integrated with renewable energy technologies (such as wind and solar) to achieve carbon neutrality goals.

First, ammonia is an excellent hydrogen carrier, and hydrogen energy is considered a crucial component of future clean energy systems. However, the storage and transportation costs of hydrogen gas at ambient temperature and pressure are prohibitively high. Ammonia has a high hydrogen density, is easily liquefied, and possesses good stability, making it an effective carrier for hydrogen. Hydrogen can be released through ammonia decomposition, providing clean fuel and creating new pathways for the global transport and large-scale application of hydrogen energy. Moreover, ammonia itself is a carbon-free fuel that does not produce carbon dioxide during combustion. This positions ammonia as a promising alternative fuel in fields such as shipping and power plants, helping to reduce greenhouse gas emissions. Ammonia fuel cells and ammonia-combustion technologies are rapidly advancing, providing technical support for the direct use of ammonia in energy systems. The existing infrastructure for ammonia is also relatively mature, especially in the fertilizer industry, where a well-established global ammonia-storage and -transport network provides a solid foundation for its application in future energy systems.

Traditional ammonia-production methods (like the Haber–Bosch process) rely on fossil fuels, resulting in high carbon emissions. In the future, using renewable energy-driven electrolysis to produce hydrogen, combined with nitrogen to synthesize ammonia, will enable the production of "green ammonia" and help achieve carbon neutrality goals. The production of green ammonia will not only help reduce the global carbon footprint but also allows for the effective storage and dispatch of renewable energy through using ammonia as an energy carrier. Future energy systems need to balance energy security, cleanliness, and economic feasibility. The multi-functionality of ammonia will enable it to play a significant role in peak shaving for the power grid, fuel substitution, and long-distance transportation, making it a key element in the future clean energy matrix. With advancements in catalytic technology, the efficiency of ammonia synthesis and utilization will further improve, making its role in the global energy transition increasingly significant.

7.2 Future research directions and development trends

Future research directions for ammonia will mainly focus on the following areas:

(1) Green synthesis technologies: ammonia synthesis typically relies on the high-temperature and high-pressure Haber–Bosch process, which is energy-intensive and results in significant carbon emissions. Future research will focus on exploring various green synthesis technologies to achieve sustainability and environmental friendliness in ammonia production. However, the scalability of current green ammonia synthesis technologies involves many factors, such as the reaction efficiency, energy consumption, equipment costs, and compatibility with existing industrial systems. Thermal catalytic ammonia synthesis, suited for large-scale production, should

integrate pressure and heat-recovery technologies to improve the overall energy efficiency and reduce carbon emissions. Plasma-catalyzed ammonia synthesis could be advantageous in distributed production systems, especially in locations with low energy costs, such as areas near renewable energy-generation sites. Although electrocatalytic and photocatalytic ammonia synthesis currently have low efficiencies, their flexible nature makes them suitable for integration with other low-carbon power-driven technologies to enhance production stability and applicability, especially in remote areas or regions with unstable energy supplies. The integrated application of these green synthesis technologies can reduce carbon emissions from ammonia production while improving its economic viability and environmental friendliness.

(2) Ammonia fuel cell technology: ammonia fuel cells, as an emerging technology, can generate electricity efficiently while reducing environmental pollution. Future research will focus on improving the energy-conversion efficiency, extending the lifespan, and reducing the costs of ammonia fuel cells. Additionally, more efficient catalysts need to be developed to promote the decomposition reaction of ammonia and enhance the overall performance of ammonia fuel cells.

(3) Ammonia cracking for hydrogen-production technology: innovations in ammonia-decomposition technology are one of the key challenges in promoting ammonia's role as a hydrogen carrier in energy systems. Although traditional high-temperature decomposition methods are effective, their high energy consumption limits the feasibility of their large-scale applications. To address this issue, research is shifting toward developing efficient catalysts that can operate at lower temperatures, which will not only reduce the reaction energy consumption but also increase the hydrogen-production rate. At the same time, the durability and poison resistance of the catalysts are also critical and need further optimization to ensure efficient performance during long-term operation. By improving the catalytic materials and optimizing the reaction conditions, future ammonia-decomposition technologies could be expected to achieve more cost-effective hydrogen production.

(4) Optimization of ammonia-storage and -transportation technologies: ammonia has certain advantages in storage and transportation compared to hydrogen, but there is still a need for further improvements in safety and costs in the future. Designing safer ammonia-storage materials and containers, and developing new ammonia-storage materials or coatings to enhance the safety and economy of storage systems, especially for long-distance transportation, is essential. Establishing an international energy-transport network based on ammonia will ensure that ammonia can flow efficiently as an energy carrier across different regions and countries in the future.

(5) Environmental impact assessment and management: although ammonia use has many potential advantages, it may also pose environmental risks during its production and use, such as ammonia leakage and its impact on ecosystems. Future research should focus on assessing the environmental impacts of ammonia throughout its entire life cycle and developing corresponding management strategies to mitigate any potential negative effects.

7.3 Interdisciplinary collaboration and future development strategies

The synthesis and utilization of ammonia is a complex system that involves multiple fields, including chemical engineering, materials science, environmental science, and energy technology. To promote advancements in ammonia technology and realize its potential in future energy systems, interdisciplinary collaboration and innovative strategies are necessary. The optimization and application of ammonia technology depend not only on breakthroughs in a single discipline but also on close collaboration among chemistry, engineering, materials, and environmental sciences. Future research needs to continuously drive technological innovations, including developing novel catalysts, optimizing reaction conditions, and exploring new green synthesis methods. Innovation is not limited to technology itself but also includes research methodologies and engineering practices. For instance, incorporating artificial intelligence and data analysis techniques can optimize catalyst design and reaction processes, enhancing production efficiency and economic viability. Also, the development of ammonia technology is not just a national or regional issue but a global challenge. International cooperation can facilitate technological exchange and resource sharing, driving technological advancement and widespread application on a global scale. Through international collaboration, the promotion and application of technologies can be accelerated, enabling a collective response to global energy and environmental challenges.

8 Conclusions

The synthesis and utilization of ammonia occupy an important position in current and future energy systems, encompassing various aspects, such as green synthesis technologies, applications, transportation, hydrogen storage, environmental impacts, and carbon reduction potential. Research on green ammonia synthesis technologies is progressing rapidly, including electrocatalytic synthesis, solar-driven synthesis, plasma catalysis, and biocatalytic synthesis. These technologies can significantly reduce carbon emissions in ammonia production, promoting environmentally friendly development. The application of ammonia in the energy sector is also expanding, as its role as a hydrogen carrier and low-carbon fuel has been validated in hydrogen fuel cells and combustion power generation. Although liquid-ammonia storage and transportation have relative advantages, safety and cost issues still need to be addressed. As an effective storage medium for hydrogen, ammonia cracking technology supports the development of the hydrogen economy. Regarding environmental impacts, while green technologies reduce the carbon footprint, a comprehensive assessment of ammonia's production and use effects is still necessary, along with the development of effective management strategies to minimize any negative impacts. In the future, further developments of ammonia will need to rely on interdisciplinary collaboration and innovation. Combined with catalyst optimization, advancements in storage technology, and policy support, ammonia is expected to play a greater role in the global energy transition and further sustainable development.

Data availability

No new data were generated or analyzed in this review article.

Conflicts of interest

The authors declare no competing interests.

Acknowledgements

This work was financially supported by the Natural Science Foundation of Jilin Province (grant no. 20240101177JC and 20240302098GX), the National Natural Science Foundation (NSFC) of China (grant no. 22379050 and 22409070), the National Key Research and Development Program of China (2023YFA1506303), and the Fundamental Research Funds for the Central Universities.

Notes and references

1 J. G. Chen, R. M. Crooks, L. C. Seefeldt, K. L. Bren, R. M. Bullock, M. Y. Darensbourg, P. L. Holland, B. Hoffman, M. J. Janik, A. K. Jones, M. G. Kanatzidis, P. King, K. M. Lancaster, S. V. Lymar, P. Pfromm, W. F. Schneider and R. R. Schrock, *Science*, 2018, **360**, eaar6611.

2 H. Zhang, L. Wang, J. Van herle, F. Maréchal and U. Desideri, *Appl. Energy*, 2020, **259**, 114135.

3 B. Lin, T. Wiesner and M. Malmali, *ACS Sustainable Chem. Eng.*, 2020, **8**, 15517–15531.

4 D. Ye and S. C. E. Tsang, *Nat. Synth.*, 2023, **2**, 612–623.

5 N. Bora, A. Kumar Singh, P. Pal, U. Kumar Sahoo, D. Seth, D. Rathore, S. Bhadra, S. Sevda, V. Venkatramanan, S. Prasad, A. Singh, R. Kataki and P. Kumar Sarangi, *Fuel*, 2024, **369**, 131808.

6 O. A. Ojelade, S. F. Zaman and B.-J. Ni, *J. Environ. Manage.*, 2023, **342**, 118348.

7 J. Guo and P. Chen, *Chem*, 2017, **3**, 709–712.

8 K. E. Lamb, M. D. Dolan and D. F. Kennedy, *Int. J. Hydrogen Energy*, 2019, **44**, 3580–3593.

9 M. Aziz, A. T. Wijayanta and A. B. Nandiyanto, *Energies*, 2020, **13**, 3062.

10 E. Rivard, M. Trudeau and K. Zaghib, *Materials*, 2019, **12**, 1973.

11 F. B. Juangsa, A. R. Irhamna and M. Aziz, *Int. J. Hydrogen Energy*, 2021, **46**, 14455–14477.

12 J. W. Erisman, M. A. Sutton, J. Galloway, Z. Klimont and W. Winiwarter, *Nat. Geosci.*, 2008, **1**, 636–639.

13 S. Giddey, S. P. S. Badwal, C. Munnings and M. Dolan, *ACS Sustainable Chem. Eng.*, 2017, **5**, 10231–10239.

14 N. Morlanés, S. P. Katikaneni, S. N. Paglieri, A. Harale, B. Solami, S. M. Sarathy and J. Gascon, *Chem. Eng. J.*, 2021, **408**, 127310.

15 Y. Kong, C. Yang, Y. Cai, X. Mu and L. Li, *Photocatal. res. potential*, 2023, **1**, 10005.

16 H. Liu, *Chin. J. Catal.*, 2014, **35**, 1619–1640.

17 A. J. Medford, A. Vojvodic, J. S. Hummelshøj, J. Voss, F. Abild-Pedersen, F. Studt, T. Bligaard, A. Nilsson and J. K. Nørskov, *J. Catal.*, 2015, **328**, 36–42.

18 S. Zhang, Y. Zhao, R. Shi, G. I. N. Waterhouse and T. Zhang, *EnergyChem*, 2019, **1**, 100013.

19 X. Cui, C. Tang and Q. Zhang, *Adv. Energy Mater.*, 2018, **8**, 1800369.

20 D. V. Yandulov and R. R. Schrock, *Science*, 2003, **301**, 76–78.

21 C. Liu, Q. Li, J. Zhang, Y. Jin, D. R. MacFarlane and C. Sun, *J. Mater. Chem. A*, 2019, **7**, 4771–4776.

22 C. Ling, X. Niu, Q. Li, A. Du and J. Wang, *J. Am. Chem. Soc.*, 2018, **140**, 14161–14168.

23 J. Zheng, F. Liao, S. Wu, G. Jones, T. Y. Chen, J. Fellowes, T. Sudmeier, I. J. McPherson, I. Wilkinson and S. C. E. Tsang, *Angew Chem. Int. Ed. Engl.*, 2019, **58**, 17335–17341.

24 P. Wang, F. Chang, W. Gao, J. Guo, G. Wu, T. He and P. Chen, *Nat. Chem.*, 2017, **9**, 64–70.

25 T. N. Ye, S. W. Park, Y. Lu, J. Li, M. Sasase, M. Kitano, T. Tada and H. Hosono, *Nature*, 2020, **583**, 391–395.

26 C. Mao, J. Wang, Y. Zou, G. Qi, J. Y. Yang Loh, T. Zhang, M. Xia, J. Xu, F. Deng, M. Ghoussoub, N. P. Kherani, L. Wang, H. Shang, M. Li, J. Li, X. Liu, Z. Ai, G. A. Ozin, J. Zhao and L. Zhang, *J. Am. Chem. Soc.*, 2020, **142**, 17403–17412.

27 M. Kitano, Y. Inoue, Y. Yamazaki, F. Hayashi, S. Kanbara, S. Matsuishi, T. Yokoyama, S. W. Kim, M. Hara and H. Hosono, *Nat. Chem.*, 2012, **4**, 934–940.

28 K. Zhang, A. Cao, L. H. Wandall, J. Vernieres, J. Kibsgaard, J. K. Nørskov and I. Chorkendorff, *Science*, 2024, **383**, 1357–1363.

29 Z. Li, Y. Lu, J. Li, M. Xu, Y. Qi, S.-W. Park, M. Kitano, H. Hosono, J.-S. Chen and T.-N. Ye, *Nat. Commun.*, 2023, **14**, 6373.

30 Y. Lu, T. N. Ye, J. Li, Z. Li, H. Guan, M. Sasase, Y. Niwa, H. Abe, Q. Li, F. Pan, M. Kitano and H. Hosono, *Angew. Chem., Int. Ed.*, 2022, **61**, e202211759.

31 T.-N. Ye, S.-W. Park, Y. Lu, J. Li, J. Wu, M. Sasase, M. Kitano and H. Hosono, *J. Am. Chem. Soc.*, 2021, **143**, 12857–12866.

32 Z. Gao, R. Tan, Z. Pan, J. Li, Q. Zhan, Z. Li, Q. Xiong, X. Mu and L. Li, *Green Chem.*, 2022, **24**, 7584–7591.

33 K.-i. Aika, H. Hori and A. Ozaki, *J. Catal.*, 1972, **27**, 424–431.

34 T. W. Hansen, J. B. Wagner, P. L. Hansen, S. Dahl, H. Topsøe and C. J. H. Jacobsen, *Science*, 2001, **294**, 1508–1510.

35 G. Ertl, *Angew Chem. Int. Ed. Engl.*, 2008, **47**, 3524–3535.

36 J. L. Dye, *Acc. Chem. Res.*, 2009, **42**, 1564–1572.

37 M. Kitano, Y. Inoue, H. Ishikawa, K. Yamagata, T. Nakao, T. Tada, S. Matsuishi, T. Yokoyama, M. Hara and H. Hosono, *Chem. Sci.*, 2016, **7**, 4036–4043.

38 Y. Lu, J. Li, T. Tada, Y. Toda, S. Ueda, T. Yokoyama, M. Kitano and H. Hosono, *J. Am. Chem. Soc.*, 2016, **138**, 3970–3973.

39 J. Wu, J. Li, Y. Gong, M. Kitano, T. Inoshita and H. Hosono, *Angew Chem. Int. Ed. Engl.*, 2019, **58**, 825–829.

40 A. Cao, V. J. Bukas, V. Shadravan, Z. Wang, H. Li, J. Kibsgaard, I. Chorkendorff and J. K. Nørskov, *Nat. Commun.*, 2022, **13**, 2382.

41 G. Xu, C. Cai and T. Wang, *J. Am. Chem. Soc.*, 2022, **144**, 23089–23095.

42 H. Yan, W. Gao, Q. Wang, Y. Guan, S. Feng, H. Wu, Q. Guo, H. Cao, J. Guo and P. Chen, *J. Phys. Chem. C*, 2021, **125**, 6716–6722.

43 Z. Liu, Q. Yu, H. Wang, J. Wu and S. Tao, *Int. J. Hydrogen Energy*, 2023, **48**, 4035–4051.

44 J. Fan, W. Li, S. Li and J. Yang, *Adv. Sci.*, 2022, **9**, 2202811.

45 S. Abanades, B. Rebiere, M. Drobek and A. Julbe, *Chem. Eng. Sci.*, 2024, **283**, 119406.

46 Y. Goto, A. Daisley and J. S. J. Hargreaves, *Catal. Today*, 2021, **364**, 196–201.

47 W. Gao, J. Guo, P. Wang, Q. Wang, F. Chang, Q. Pei, W. Zhang, L. Liu and P. Chen, *Nat. Energy*, 2018, **3**, 1067–1075.

48 B. Wang and L. Shen, *Ind. Eng. Chem. Res.*, 2022, **61**, 18215–18231.

49 S. Laassiri, C. D. Zeinalipour-Yazdi, C. R. A. Catlow and J. S. J. Hargreaves, *Appl. Catal., B*, 2018, **223**, 60–66.

50 S. Laassiri, C. D. Zeinalipour-Yazdi, N. Bion, C. R. A. Catlow and J. S. J. Hargreaves, *Faraday Discuss.*, 2021, **229**, 281–296.

51 X. Zhang, C. Pei, X. Chang, S. Chen, R. Liu, Z.-J. Zhao, R. Mu and J. Gong, *J. Am. Chem. Soc.*, 2020, **142**, 11540–11549.

52 B. Wang, H. Guo, X. Yin and L. Shen, *Energy Fuels*, 2020, **34**, 10247–10255.

53 B. Wang, X. Yin, P. Wang and L. Shen, *Int. J. Hydrogen Energy*, 2023, **48**, 2705–2717.

54 T. Yamaguchi, K. Shinzato, K. Yamamoto, Y. Wang, Y. Nakagawa, S. Isobe, T. Ichikawa, H. Miyaoka and T. Ichikawa, *Int. J. Hydrogen Energy*, 2020, **45**, 6806–6812.

55 S. Brown, B. Robinson, Y. Wang, C. Wildfire and J. Hu, *J. Mater. Chem. A*, 2022, **10**, 15497–15507.

56 Q. Lai, T. Cai, S. C. E. Tsang, X. Chen, R. Ye, Z. Xu, M. D. Argyle, D. Ding, Y. Chen, J. Wang, A. G. Russell, Y. Wu, J. Liu and M. Fan, *Sci. Bull.*, 2022, **67**, 2124–2138.

57 P. Mehta, P. Barboun, F. A. Herrera, J. Kim, P. Rumbach, D. B. Go, J. C. Hicks and W. F. Schneider, *Nat. Catal.*, 2018, **1**, 269–275.

58 Y. Engelmann, K. van 't Veer, Y. Gorbanev, E. C. Neyts, W. F. Schneider and A. Bogaerts, *ACS Sustainable Chem. Eng.*, 2021, **9**, 13151–13163.

59 H. Conrads and M. Schmidt, *Plasma Sources Sci. Technol.*, 2000, **9**, 441.

60 J. Hong, S. Prawer and A. B. Murphy, *ACS Sustainable Chem. Eng.*, 2018, **6**, 15–31.

61 P. Mehta, P. M. Barboun, Y. Engelmann, D. B. Go, A. Bogaerts, W. F. Schneider and J. C. Hicks, *ACS Catal.*, 2020, **10**, 6726–6734.

62 J. N. Galloway, A. R. Townsend, J. W. Erisman, M. Bekunda, Z. Cai, J. R. Freney, L. A. Martinelli, S. P. Seitzinger and M. A. Sutton, *Science*, 2008, **320**, 889–892.

63 G. Akay and K. Zhang, *Ind. Eng. Chem. Res.*, 2017, **56**, 457–468.

64 A. Gómez-Ramírez, J. Cotrino, R. M. Lambert and A. R. González-Elipe, *Plasma Sources Sci. Technol.*, 2015, **24**, 065011.

65 M. Iwamoto, M. Akiyama, K. Aihara and T. Deguchi, *ACS Catal.*, 2017, **7**, 6924–6929.

66 J. Shah, W. Wang, A. Bogaerts and M. L. Carreon, *ACS Appl. Energy Mater.*, 2018, **1**, 4824–4839.

67 J. Shah, J. Harrison and M. Carreon, *Catalysts*, 2018, **8**, 437.

68 H.-H. Kim, Y. Teramoto, A. Ogata, H. Takagi and T. Nanba, *Plasma Processes Polym.*, 2017, **14**, 1600157.

69 Y. Liu, C. W. Wang, X. F. Xu, B. W. Liu, G. M. Zhang, Z. W. Liu, Q. Chen and H. B. Zhang, *Plasma Chem. Plasma Process.*, 2022, **42**, 267–282.

70 B. S. Patil, A. S. R. van Kaathoven, F. J. J. Peeters, N. Cherkasov, J. Lang, Q. Wang and V. Hessel, *J. Phys. D: Appl. Phys.*, 2020, **53**, 144003.

71 X. Hu, X. Zhu, X. Wu, Y. Cai and X. Tu, *Plasma Processes Polym.*, 2020, **17**, DOI: 10.1002/ppap.202000072.

72 Y. Wang, M. Craven, X. Yu, J. Ding, P. Bryant, J. Huang and X. Tu, *ACS Catal.*, 2019, **9**, 10780–10793.

73 J. R. Shah, F. Gorky, J. Lucero, M. A. Carreon and M. L. Carreon, *Ind. Eng. Chem. Res.*, 2020, **59**, 5167–5176.

74 F. Gorky, J. M. Lucero, J. M. Crawford, B. Blake, M. A. Carreon and M. L. Carreon, *ACS Appl. Mater. Interfaces*, 2021, **13**, 21338–21348.

75 S. Li, Y. Shao, H. Chen and X. Fan, *Ind. Eng. Chem. Res.*, 2022, **61**, 3292–3302.

76 Y. Wang, W. Yang, S. Xu, S. Zhao, G. Chen, A. Weidenkaff, C. Hardacre, X. Fan, J. Huang and X. Tu, *J. Am. Chem. Soc.*, 2022, **144**, 12020–12031.

77 P. Navascués, J. M. Obrero-Pérez, J. Cotrino, A. R. González-Elipe and A. Gómez-Ramírez, *ACS Sustainable Chem. Eng.*, 2020, **8**, 14855–14866.

78 A. Gómez-Ramírez, A. M. Montoro-Damas, J. Cotrino, R. M. Lambert and A. R. González-Elipe, *Plasma Processes Polym.*, 2016, **14**, DOI: 10.1002/ppap.201600081.

79 P. Navascués, J. Garrido-García, J. Cotrino, A. R. González-Elipe and A. Gómez-Ramírez, *ACS Sustainable Chem. Eng.*, 2023, **11**, 3621–3632.

80 K. H. R. Rouwenhorst, H.-H. Kim and L. Lefferts, *ACS Sustainable Chem. Eng.*, 2019, **7**, 17515–17522.

81 H. Wu, L. Yang, J. Wen, Y. Xu, Y. Cai, W. Gao, Q. Wang, Y. Guan, S. Feng, H. Cao, T. He, L. Liu, S. Zhang, J. Guo and P. Chen, *Adv. Energy Mater.*, 2023, **13**, 2300722.

82 B. N. Bayer, P. J. Bruggeman and A. Bhan, *ACS Catal.*, 2023, **13**, 2619–2630.

83 M. Liu, Y. Yi, L. Wang, H. Guo and A. Bogaerts, *Catalysts*, 2019, **9**, 275.

84 Y.-R. Zhang, K. Van Laer, E. C. Neyts and A. Bogaerts, *Appl. Catal., B*, 2016, **185**, 56–67.

85 X. Chen, N. Li, Z. Kong, W.-J. Ong and X. Zhao, *Mater. Horiz.*, 2018, **5**, 9.

86 Y. Shi, Z. Zhao, D. Yang, J. Tan, X. Xin, Y. Liu and Z. Jiang, *Chem. Soc. Rev.*, 2023, **52**, 6938–6956.

87 G. N. Schrauzer and T. D. Guth, *J. Am. Chem. Soc.*, 1977, **99**, 7189–7193.
88 R. Fu, Z. Wu, Z. Pan, Z. Gao, Z. Li, X. Kong and L. Li, *Angew Chem. Int. Ed. Engl.*, 2021, **60**, 11173–11179.
89 C. Liu, D. Hao, J. Ye, S. Ye, F. Zhou, H. Xie, G. Qin, J. Xu, J. Liu, S. Li and C. Sun, *Adv. Energy Mater.*, 2023, **13**, 2204126.
90 X. Xue, R. Chen, H. Chen, Y. Hu, Q. Ding, Z. Liu, L. Ma, G. Zhu, W. Zhang, Q. Yu, J. Liu, J. Ma and Z. Jin, *Nano Lett.*, 2018, **18**, 7372–7377.
91 Z. Zhao, R. Tan, Y. Kong, Z. Zhang, S. Qiu, X. Mu and L. Li, *Angew Chem. Int. Ed. Engl.*, 2023, **62**, e202303629.
92 G. Zhang, X. Yang, C. He, P. Zhang and H. Mi, *J. Mater. Chem. A*, 2020, **8**, 334–341.
93 Z. Li, Z. Gao, B. Li, L. Zhang, R. Fu, Y. Li, X. Mu and L. Li, *Appl. Catal., B*, 2020, **262**, 118276.
94 L. Li, Y. Wang, S. Vanka, X. Mu, Z. Mi and C. J. Li, *Angew Chem. Int. Ed. Engl.*, 2017, **56**, 8701–8705.
95 Y. Guan, H. Wen, K. Cui, Q. Wang, W. Gao, Y. Cai, Z. Cheng, Q. Pei, Z. Li, H. Cao, T. He, J. Guo and P. Chen, *Nat. Chem.*, 2024, **16**, 373–379.
96 R. Li, W. Ma, Y. Liu, L. Zhang and Z. Zhou, *J. Mater. Chem. A*, 2023, **11**, 18626–18645.
97 S. L. Foster, S. I. P. Bakovic, R. D. Duda, S. Maheshwari, R. D. Milton, S. D. Minteer, M. J. Janik, J. N. Renner and L. F. Greenlee, *Nat. Catal.*, 2018, **1**, 490–500.
98 Z. Huang, B. Yang, Y. Zhou, W. Luo, G. Chen, M. Liu, X. Liu, R. Ma and N. Zhang, *ACS Nano*, 2023, **17**, 25091–25100.
99 A. R. Singh, B. A. Rohr, J. A. Schwalbe, M. Cargnello, K. Chan, T. F. Jaramillo, I. Chorkendorff and J. K. Nørskov, *ACS Catal.*, 2017, **7**, 706–709.
100 A. Tsuneto, A. Kudo and T. Sakata, *Chem. Lett.*, 1993, **22**, 851–854.
101 K. Kim, S. J. Lee, D.-Y. Kim, C.-Y. Yoo and J. W. Choi, *ChemSusChem*, 2018, **11**(1), 120–124.
102 N. Lazouski, M. Chung, K. Williams, M. L. Gala and K. Manthiram, *Nat. Catal.*, 2020, **3**, 463–469.
103 X. Yu, P. Han, Z. Wei, L. Huang, Z. Gu, S. Peng, J. Ma and G. Zheng, *Joule*, 2018, **2**, 1610–1622.
104 S. Li, Y. Zhou, X. Fu, J. B. Pedersen, M. Saccoccio, S. Z. Andersen, K. Enemark-Rasmussen, P. J. Kempen, C. D. Damsgaard, A. Xu, R. Sažinas, J. B. V. Mygind, N. H. Deissler, J. Kibsgaard, P. C. K. Vesborg, J. K. Nørskov and I. Chorkendorff, *Nature*, 2024, **629**, 92–97.
105 X. Fu, V. A. Niemann, Y. Zhou, S. Li, K. Zhang, J. B. Pedersen, M. Saccoccio, S. Z. Andersen, K. Enemark-Rasmussen, P. Benedek, A. Xu, N. H. Deissler, J. B. V. Mygind, A. C. Nielander, J. Kibsgaard, P. C. K. Vesborg, J. K. Nørskov, T. F. Jaramillo and I. Chorkendorff, *Nat. Mater.*, 2024, **23**, 101–107.
106 Y. Li, Q. Zhang, Z. Mei, S. Li, W. Luo, F. Pan, H. Liu and S. Dou, *Small Methods*, 2021, **5**, 2100460.
107 X. Wang, S. Sun, J. Yao, H. Wan, R. Ma and W. Ma, *Energy Environ. Mater.*, 2024, **7**, e12709.
108 A. J. Reiter and S.-C. Kong, *Fuel*, 2011, **90**, 87–97.
109 C. Zamfirescu and I. Dincer, *Fuel Process. Technol.*, 2009, **90**, 729–737.
110 W. Wang, J. M. Herreros, A. Tsolakis and A. P. E. York, *Int. J. Hydrogen Energy*, 2013, **38**, 9907–9917.
111 W. H. Avery, *Int. J. Hydrogen Energy*, 1988, **13**, 761–773.
112 N. Salmon and R. Bañares-Alcántara, *Sustainable Energy Fuels*, 2021, **5**, 2814.
113 E. Martinez-Ahumada, M. L. Diaz-Ramirez, M. J. Velasquez-Hernandez, V. Jancik and I. A. Ibarra, *Chem. Sci.*, 2021, **12**, 6772–6799.
114 C. H. C. R. Z. Sørensen, T. Johannessen, U. J. Quaade, K. Honkala, T. D. Elmøe, R. Køhler and J. K. Nørskov, *J. Mater. Chem.*, 2005, **15**, 4106–4109.
115 J. Helminen, J. Helenius, E. Paatero and I. Turunen, *J. Chem. Eng. Data*, 2001, **46**, 391–399.
116 A. M. B. Furtado, Y. Wang, T. G. Glover and M. D. LeVan, *Microporous Mesoporous Mater.*, 2011, **142**, 730–739.
117 T. Islamoglu, Z. Chen, M. C. Wasson, C. T. Buru, K. O. Kirlikovali, U. Afrin, M. R. Mian and O. K. Farha, *Chem. Rev.*, 2020, **120**, 8130–8160.
118 M. Jahandar Lashaki, S. Khiavi and A. Sayari, *Chem. Soc. Rev.*, 2019, **48**, 3320–3405.
119 P. J. Waller, F. Gándara and O. M. Yaghi, *Acc. Chem. Res.*, 2015, **48**, 3053–3063.
120 S. Das, P. Heasman, T. Ben and S. Qiu, *Chem. Rev.*, 2017, **117**, 1515–1563.
121 H. Ishaq and C. Crawford, *Energy Convers. Manage.*, 2024, **300**, 117869.
122 Y. Sui, A. Abdulkreem Al-Huqail, M. Suhatril, A. M. Abed, Y. Zhao, H. Assilzadeh, M. Amine Khadimallah and H. Elhosiny Ali, *Fuel*, 2023, **331**, 125685.
123 D. J. Durbin and C. Malardier-Jugroot, *Int. J. Hydrogen Energy*, 2013, **38**, 14595–14617.
124 F. Zhang, P. Zhao, M. Niu and J. Maddy, *Int. J. Hydrogen Energy*, 2016, **41**, 14535–14552.
125 A. Klerke, C. H. Christensen, J. K. Nørskov and T. Vegge, *J. Mater. Chem.*, 2008, **18**, 2304–2310.
126 A. Valera-Medina, H. Xiao, M. Owen-Jones, W. I. F. David and P. J. Bowen, *Prog. Energy Combust. Sci.*, 2018, **69**, 63–102.
127 L. Miron, R. Chiriac, M. Brabec and V. Bădescu, *Energy Rep.*, 2021, **7**, 5483–5494.
128 A. A. Konnov, A. Mohammad, V. R. Kishore, N. I. Kim, C. Prathap and S. Kumar, *Prog. Energy Combust. Sci.*, 2018, **68**, 197–267.
129 R. C. Murray and A. R. Hall, *Trans. Faraday Soc.*, 1951, **47**, 743–751.
130 J. A. Miller and C. T. Bowman, *Prog. Energy Combust. Sci.*, 1989, **15**, 287–338.
131 R. K. Lyon and J. E. Hardy, *Ind. Eng. Chem. Fundam.*, 1986, **25**, 19–24.
132 R. P. Lindstedt, F. C. Lockwood and M. A. Selim, *Combust. Sci. Technol.*, 1994, **99**, 253–276.
133 J. A. Miller, M. D. Smooke, R. M. Green and R. J. Kee, *Combust. Sci. Technol.*, 1983, **34**, 149–176.
134 J. Bian, J. Vandooren and P. J. Van Tiggelen, *Symp. (Int.) Combust., [Proc.]*, 1988, **21**, 953–963.
135 J. Otomo, M. Koshi, T. Mitsumori, H. Iwasaki and K. Yamada, *Int. J. Hydrogen Energy*, 2018, **43**, 3004–3014.

136 W. S. Chai, Y. Bao, P. Jin, G. Tang and L. Zhou, *Renewable Sustainable Energy Rev.*, 2021, **147**, 111254.

137 A. M. Abdalla, S. Hossain, A. T. Azad, P. M. I. Petra, F. Begum, S. G. Eriksson and A. K. Azad, *Renewable Sustainable Energy Rev.*, 2018, **82**, 353–368.

138 A. Kirubakaran, S. Jain and R. K. Nema, *Renewable Sustainable Energy Rev.*, 2009, **13**, 2430–2440.

139 A. Valera-Medina, F. Amer-Hatem, A. K. Azad, I. C. Dedoussi, M. de Joannon, R. X. Fernandes, P. Glarborg, H. Hashemi, X. He, S. Mashruk, J. McGowan, C. Mounaim-Rouselle, A. Ortiz-Prado, A. Ortiz-Valera, I. Rossetti, B. Shu, M. Yehia, H. Xiao and M. Costa, *Energy Fuels*, 2021, **35**, 6964–7029.

140 K. T. Møller, T. R. Jensen, E. Akiba and H.-w. Li, *Prog. Nat. Sci.: Mater. Int.*, 2017, **27**, 34–40.

141 A. Afif, N. Radenahmad, Q. Cheok, S. Shams, J. H. Kim and A. K. Azad, *Renewable Sustainable Energy Rev.*, 2016, **60**, 822–835.

142 A. Yapicioglu and I. Dincer, *Renewable Sustainable Energy Rev.*, 2019, **103**, 96–108.

143 B. C. H. Steele and A. Heinzel, *Nature*, 2001, **414**, 345–352.

144 N. Q. Minh, *J. Am. Ceram. Soc.*, 1993, **76**, 563–588.

145 N. M. Adli, H. Zhang, S. Mukherjee and G. Wu, *J. Electrochem. Soc.*, 2018, **165**, J3130–J3147.

146 J. C. Ganley, *J. Power Sources*, 2008, **178**, 44–47.

147 C. Zhong, W. B. Hu and Y. F. Cheng, *J. Mater. Chem. A*, 2013, **1**, 3216–3238.

148 C. G. Vayenas and R. D. Farr, *Science*, 1980, **208**, 593–594.

149 A. Wojcik, H. Middleton, I. Damopoulos and J. Van herle, *J. Power Sources*, 2003, **118**, 342–348.

150 M. Ni, M. K. H. Leung and D. Y. C. Leung, *Energy Convers. Manage.*, 2008, **49**, 2748–2756.

151 G. G. M. Fournier, I. W. Cumming and K. Hellgardt, *J. Power Sources*, 2006, **162**, 198–206.

152 G. Jeerh, M. Zhang and S. Tao, *J. Mater. Chem. A*, 2021, **9**, 727–752.

153 M. Kishimoto, N. Furukawa, T. Kume, H. Iwai and H. Yoshida, *Int. J. Hydrogen Energy*, 2017, **42**, 2370–2380.

154 A. Boisen, S. Dahl, J. K. Nørskov and C. H. Christensen, *J. Catal.*, 2005, **230**, 309–312.

155 C. Chen, K. Wu, H. Ren, C. Zhou, Y. Luo, L. Lin, C. Au and L. Jiang, *Energy Fuels*, 2021, **35**, 11693–11706.

156 J. C. Ganley, F. S. Thomas, E. G. Seebauer and R. I. Masel, *Catal. Lett.*, 2004, **96**, 117–122.

157 Y. Yi, L. Wang, Y. Guo, S. Sun and H. Guo, *AlChE J.*, 2019, **65**, 691–701.

158 S. Shetty, A. P. J. Jansen and R. A. van Santen, *J. Phys. Chem. C*, 2008, **112**, 17768–17771.

159 S. J. Wang, S. F. Yin, L. Li, B. Q. Xu, C. F. Ng and C. T. Au, *Appl. Catal., B*, 2004, **52**, 287–299.

160 T. Su, B. Guan, J. Zhou, C. Zheng, J. Guo, J. Chen, Y. Zhang, Y. Yuan, W. Xie, N. Zhou, H. Dang, B. Xu and Z. Huang, *Energy Fuels*, 2023, **37**, 8099–8127.

161 Q. Su, L. Gu, Y. Yao, J. Zhao, W. Ji, W. Ding and C.-T. Au, *Appl. Catal., B*, 2017, **201**, 451–460.

162 H. Fang, S. Wu, T. Ayvali, J. Zheng, J. Fellowes, P.-L. Ho, K. C. Leung, A. Large, G. Held, R. Kato, K. Suenaga, Y. I. A. Reyes, H. V. Thang, H.-Y. T. Chen and S. C. E. Tsang, *Nat. Commun.*, 2023, **14**, 647.

163 K. C. Leung, S. Hong, G. Li, Y. Xing, B. K. Y. Ng, P.-L. Ho, D. Ye, P. Zhao, E. Tan, O. Safonova, T.-S. Wu, M. M.-J. Li, G. Mpourmpakis and S. C. E. Tsang, *J. Am. Chem. Soc.*, 2023, **145**, 14548–14561.

164 H. Tabassum, S. Mukherjee, J. Chen, D. Holiharimanana, S. Karakalos, X. Yang, S. Hwang, T. Zhang, B. Lu, M. Chen, Z. Tang, E. A. Kyriakidou, Q. Ge and G. Wu, *Energy Environ. Sci.*, 2022, **15**, 4190–4200.

165 A. M. Karim, V. Prasad, G. Mpourmpakis, W. W. Lonergan, A. I. Frenkel, J. G. Chen and D. G. Vlachos, *J. Am. Chem. Soc.*, 2009, **131**, 12230–12239.

166 F. Hayashi, Y. Toda, Y. Kanie, M. Kitano, Y. Inoue, T. Yokoyama, M. Hara and H. Hosono, *Chem. Sci.*, 2013, **4**, 3124–3130.

167 Z. Wang, Z. Cai and Z. Wei, *ACS Sustainable Chem. Eng.*, 2019, **7**, 8226–8235.

168 Y. Zhang, J. Li, Y. Zhou, C.-t. Au, X. Wang and L. Jiang, *Fundam. Res.*, 2024, DOI: **10.1016/j.fmre.2023.11.016**.

169 G.-L. Hou and E. Janssens, *Fundam. Res.*, 2023, DOI: **10.1016/j.fmre.2023.10.011**.

170 J. Tian, L. Wang, Y. Xiong, Y. Wang, W. Yin, G. Tian, Z. Wang, Y. Cheng and S. Ji, *Process Saf. Environ. Prot.*, 2024, **183**, 514–543.

171 Y. Zhao, B. P. Setzler, J. Wang, J. Nash, T. Wang, B. Xu and Y. Yan, *Joule*, 2019, **3**, 2472–2484.

172 S. Giddey, S. P. S. Badwal and A. Kulkarni, *Int. J. Hydrogen Energy*, 2013, **38**, 14576–14594.

173 C. Smith, A. K. Hill and L. Torrente-Murciano, *Energy Environ. Sci.*, 2020, **13**, 331–344.

174 B. Leighty and J. Holbrook, *Wind Eng.*, 2008, **32**, 45–66.

175 M. Al-Zareer, I. Dincer and M. A. Rosen, *Int. J. Hydrogen Energy*, 2019, **44**, 18214–18224.

176 D. Erdemir and I. Dincer, *Int. J. Energy Res.*, 2021, **45**, 4827–4834.

177 X. Sun, M. Li, J. Li, X. Duan, C. Wang, W. Luo, H. Liu and J. Liu, *Energies*, 2023, **16**, 908.

178 Z. u. Rahman, X. Wang, H. Mikulcic, S. Zhou, J. Zhang, M. Vujanovic and H. Tan, *J. Energy Inst.*, 2022, **100**, 89–98.